NASA CONTRACTOR REPORT

NASA CR-2080

THEORETICAL STUDY OF CORRUGATED PLATES: SHEARING OF A CORRUGATED PLATE WITH CURVILINEAR CORRUGATIONS

by Lung-Hsiang Wu and Charles Libove

Prepared by
SYRACUSE UNIVERSITY
Syracuse, N.Y. 13210
for Langley Research Center

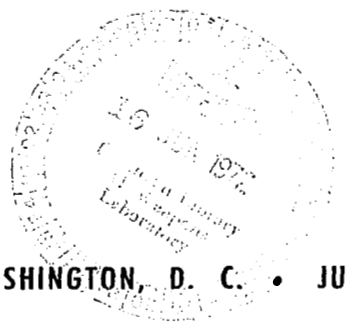

NATIONAL AERONAUTICS AND SPACE ADMINISTRATION • WASHINGTON, D. C. • JUNE 1972

1. Report No.	2. Government Accession No.	3. Recipient's Catalog No.
NASA CR-2080		

4. Title and Subtitle	5. Report Date
THEORETICAL STUDY OF CORRUGATED PLATES: SHEARING OF A CORRUGATED PLATE WITH CURVILINEAR CORRUGATIONS	JUNE 1972
	6. Performing Organization Code
7. Author(s)	8. Performing Organization Report No.
Lung-Hsiang Wu and Charles Libove	MAE 1833-T4
	10. Work Unit No.
9. Performing Organization Name and Address	134-14-05-02
Syracuse University Syracuse, New York 13210	11. Contract or Grant No.
	NGR-33-022-115
	13. Type of Report and Period Covered
12. Sponsoring Agency Name and Address	Contractor report
National Aeronautics and Space Administration Washington, D.C. 20546	14. Sponsoring Agency Code

15. Supplementary Notes

16. Abstract

A theoretical elastic analysis is presented for the in-plane shear of a corrugated plate with curvilinear corrugations and with discrete attachments between the ends of the corrugations and the surrounding members. The purpose of the analysis is to obtain information about the effective shear stiffness of the plate and the flexural strains that develop in it during the shearing process as a result of the attendant cross-sectional deformations. The crests and troughs of the corrugation cross section are assumed to be identical circular arcs. The following four kinds of discrete attachment at the corrugation ends are considered in the analysis: (a) point attachments in the troughs, (b) point attachments at the crests and in the troughs, (c) point attachments at mid-height, and (d) point attachments at mid-height, at the crests, and in the troughs.

17. Key Words (Suggested by Author(s))	18. Distribution Statement
Corrugated plates Shear webs Shear stiffness	Unclassified - Unlimited

19. Security Classif. (of this report)	20. Security Classif. (of this page)	21. No. of Pages	22. Price*
Unclassified	Unclassified	79	$3.00

*For sale by the National Technical Information Service, Springfield, Virginia 22151

CONTENTS

SUMMARY

A theoretical elastic analysis is presented for the in-plane shear of a corrugated plate with curvilinear corrugations and with discrete attachments between the ends of the corrugations and the surrounding members. The purpose of the analysis is to obtain information about the effective shear stiffness of the plate and the flexural strains that develop in it during the shearing process as a result of the attendant cross-sectional deformations.

The crests and troughs of the corrugation cross section are assumed to be identical circular arcs. The following four kinds of discrete attachment at the corrugation ends are considered in the analysis: (a) point attachments in the troughs, (b) point attachments at the crests and in the troughs, (c) point attachments at mid-height, and (d) point attachments at mid-height, at the crests, and in the troughs.

The analysis employs the method of minimum total potential energy and the calculus of variations in order to obtain differential equations and boundary conditions governing the longitudinal variation of certain assumed component modes of deformation of the cross sections, including deformations in the plane of the cross section as well as normal to the plane of the cross section. The present analysis is believed to be more accurate than a previous analysis of the same problem; in particular, it does not employ an assumption implicit in the previous analysis to the effect that the straight-line generators of the corrugation remain straight lines.

Numerical results are presented only for the first of the four kinds of end attachment listed above, but for a wide range of geometries. The numerical results show that (a) the shear stiffness of the discretely attached corrugated plate can be much lower than that of the continuously attached corrugated plate, and (b) the extreme-fiber flexural stresses in the discretely attached corrugated plate, associated with the deformations of the end cross sections in their own planes, can be very high.

INTRODUCTION

This is the fourth report in a series dealing with the elastic shearing analysis of corrugated plates having discrete rather than continuous attachments at the ends of the corrugations. The three previous reports (refs. 1, 2 and 3) dealt with corrugations of trapezoidal cross section. The present report considers corrugations of curvilinear cross section.

The objective of this report, as of the previous ones, is to arrive at means of predicting the overall in-plane shear stiffness of discretely attached corrugated plates as well as the stresses which develop in them during the shearing process. This objective is motivated by the fact that corrugated shear webs, with the corrugations running vertically, have been proposed for use in the spars of aerospace vehicles as a means of avoiding high thermal stresses due to temperature difference between the outer skin and the inner webs, and for ease of construction in such applications the attachment between the ends of the corrugations and the spar caps may be discrete rather than continuous.

For simplicity of analysis the cross section is assumed to be composed of circular arcs. It is expected, however, that the results for a cross section composed of circular arcs may be applicable, at least as an approximation, to other types of curvilinear cross section (e.g., sinusoidal) provided that they have the same pitch and height as the circular-arc cross section.

Figure 1 shows the configuration of the corrugated plate and some of the notation to be employed in connection with it. As indicated in the figure, the sheet thickness is t, and the circular arcs making up the cross section have a radius of $R(>>t)$ and a central angle of 2θ. The arcs are joined to form a wave of pitch p and height h, related to R and θ through the following equations:

$$p = 4R \sin\theta, \qquad h = 2R(1 - \cos\theta) \tag{1a}$$

Equations (1a) permit p and h to be readily evaluated if R and θ are given. On the other hand, if p and h are given, R and θ can be evaluated

from the following inverted form of equations (1a):

$$\theta = 2 \tan^{-1} \left(\frac{2h}{p}\right) \quad , \qquad R = \frac{1}{4}p \left(\frac{1}{4}\frac{p}{h} + \frac{h}{p}\right) \tag{1b}$$

Equations (1b) can also be used for finding the θ and R of a circular-arc corrugated plate having the same pitch and height as a given not-quite-circular-arc corrugated plate. (To facilitate this use of the equations they are graphed in figure 18.)

As shown in figure 1, the length of the corrugations is denoted by L or 2b. The coordinate system includes a longitudinal coordinate z, a transverse coordinate x, and a second transverse coordinate, s, measured along the cross section centerline, starting from a crest. Also as indicated in figure 1, certain generators of the corrugation will be referred to as crest lines, others as trough lines.

Four different kinds of discrete attachment will be considered at the ends of the corrugations, that is, along the edges $z = \pm b$. These are illustrated in figure 2 and may be described as follows:

(a) Point attachments at troughs only.

(b) Point attachments at troughs and crests.

(c) Point attachments at mid-height.

(d) Point attachments at troughs, crests and mid-height (combination of (b) and (c)).

In all cases the attachments are considered as mathematical points providing constraint against displacement, but not against rotation. The attachments are identical at both ends ($z = +b$, $z = -b$) of the corrugations. Except at the attachment points, there is assumed to be no interference by surrounding members with the cross-sectional deformations which may occur during the shearing of the plate.

Acknowledgement. - This work was supported by the National Aeronautics and Space Administration under grant NGR-33-022-115.

SYMBOLS

b	$L/2$ (fig. 1)
D_s	$Et^3/[12(1-\nu\nu')]$
D_{sz}	$G't^3/12$
D_z	$E't^3/[12(1-\nu\nu')]$
E, E'	Young's moduli of orthotropic material
E_z	$E'/(1-\nu\nu')$
F	shear force (fig. 1)
G, G'	shear modulus
h	height of corrugation (fig. 1)
L	length of corrugation (fig. 1)
p	pitch of the corrugation (fig. 1)
p'	developed width of one corrugation
R	radius of crests and troughs (fig. 1)
s, $\bar{s}$	transverse coordinates measured along the corrugation profile (fig. 5)
t	thickness of corrugation (fig. 1)
U	strain energy
u, $\bar{u}$	longitudinal displacement components
$2u_o$	overall shear displacement per corrugation
v, w; $\bar{v}$, $\bar{w}$	displacement components in the plane of the cross section (fig. 5)
x	transverse Cartesian coordinate (fig. 1)
z	longitudinal coordinate (fig. 1)

β, $\bar{\beta}$	rotations in the plane of the cross section (figs. 4, 5)
γ	shear strain
ε_{ℓ}	longitudinal strain
ε_{t}	transverse strain
ε_{s}	transverse strain of middle surface
ζ	thickness coordinate (fig. 6)
θ	half the central angle of a crest or trough (fig. 1)
ν, ν'	Poisson's ratio of orthotropic material
ρ	radius of curvature (fig. 4)
σ_{ℓ}	longitudinal stress
σ_{t}	transverse stress
τ	shear stress
Ω	dimensionless shear stiffness (the shear stiffness of plate with discrete attachments divided by shear stiffness of identical plate with continuous attachment)

GENERAL ANALYSIS

Mechanism of Shearing

The plate will be assumed to be composed of infinitely many corrugations, all identical, and all subjected to the same deformation. Thus, the analysis may be based on a single corrugation. By a single corrugation is meant that portion of the plate consisting of one complete wave between two corresponding generators. For convenience, the two generators defining the single corrugation will be selected from those which pass through the end attachments. Thus, in each part of figure 2 the generators labeled A and C will be taken to represent the left and right edge of the single corrugation typical of all the corrugations.

The shearing of the plate is imagined to be accomplished by imposing relative longitudinal (z-wise) shifts on those generators which pass through the attachment points, the amount of the relative shift being $2u_o$ per corrugation. Thus, for each of the cases illustrated in figure 2 the generator C is shifted longitudinally a distance $2u_o$ with respect to the generator A. Where there are attachment points between A and C, as in parts (b), (c), and (d) of figure 2, the generators passing through those points are assumed to undergo a longitudinal shift relative to A which is a fraction of $2u_o$, the fraction depending upon the location of the generator. Thus, the generator labeled B in each of figures 2(b), (c) and (d) is assumed to shift longitudinally an amount u_o relative to A. In figure 2(d) the longitudinal shift of A' with respect to A is one-fourth of $2u_o$, or $u_o/2$; that of C' with respect to A three-fourths of $2u_o$, or $3u_o/2$.

In these imposed shifts, the end points (attachment points) of the shifted generators undergo only longitudinal (z-wise)displacements; but intermediate points along these generators are free to move both longitudinally and laterally, resulting in a curving of these generators along with all the others.

As a result of the imposed shearing deformation described above, a resultant shear force F will be developed on each longitudinal cross section, as indicated in figure 1(b). The couple formed by these forces on any segment of the plate is assumed to be reacted by means of forces (not shown in fig. 1(b)) parallel to the x-axis at the attachment points along the edges $z = \pm b$.

Symmetry and Antisymmetry Properties of the Deformation

Considerations of linearity, symmetry and continuity dictate that all of the labeled middle-surface generators in figure 2, as well as any crest lines and trough lines not labeled, must have zero longitudinal strain everywhere along their lengths. Furthermore, although the crest lines and trough lines may curve in the horizontal plane, they cannot curve in vertical planes.

One can also deduce certain symmetry and antisymmetry characteristics for the displacements in the plane of the cross section. Figure 3 shows two points, a and a', both in the same cross section and one the mirror image of the other with respect to a vertical plane of symmetry of the corrugation. As implied by the upper part of figure 3, both points must experience equal horizontal displacement components, but equal and opposite vertical displacement components. Resolving the Δ_V and Δ_H at each point into normal and tangential components, one obtains the symmetry and antisymmetry properties shown in the lower part of figure 3 for those components of displacement.

Besides having the properties just discussed, the displacement components Δ_N and Δ_T in the plane of the cross section can be shown to be odd with respect to z.

Turning to the longitudinal strains, one can deduce that in a given cross section the longitudinal (z-wise) strain at any point, a, is the negative of the

longitudinal strain at its mirror-image point, a', while along a given generator the longitudinal strain is an odd function of z.

Finally, referring to figure 2, it can be argued that, except for a rigid-body motion of the entire corrugated plate, the longitudinal displacements u(s,z) of middle-surface points must be odd with respect to s.

Kinematics of the Deformation of a Cross Section in its Own Plane

In this section relationships will be developed governing the deformation of a cross section in its own plane, starting with an arbitrary cross section and then specializing to the case of the circular-arc cross section of figure 1(a).

Figure 4 represents the arbitrary cross section. Point P, with coordinate s, is a typical point on the middle surface. The local radius of curvature at this point is ρ (positive if the center of curvature is below the cross section, as shown), and α is the angle between the local normal and the vertical. The vectors $\vec{t}$ and $\vec{n}$ are local unit vectors tangential and normal to the middle surface and lying in the plane of the undeformed cross section, with $\vec{t}$ always pointing in the direction of increasing s, and $\vec{n}$ always in the direction corresponding to a 90° counterclockwise rotation of $\vec{t}$. A third unit vector $\vec{k}$, not shown, is to be imagined pointing out of the paper. The direction of $\vec{k}$ is also to be taken as the positive z direction.

Point P and the infinitely close point Q define an infinitesimal arc of length ds subtending an infinitesimal angle $d\alpha$. The vector corresponding to this arc is

$$\vec{PQ} = \vec{t}\, ds \tag{2}$$

Displacements. - The displacement of the typical point P has a longitudinal (z-wise) component and a component in the plane of the cross section. The latter component is represented in figure 4 by the displacement vector

$$\vec{U} = v\vec{t} + w\vec{n} \tag{3}$$

where $v(s,z)$ and $w(s,z)$ are the scalar components of the displacement vector in the directions of $\vec{t}$ and $\vec{n}$, respectively. The neighboring point Q will have the infinitesimally different displacement component $\vec{U} + (\partial\vec{U}/\partial s)ds$ in the plane of the cross section, where, from equation (3),

$$\frac{\partial \vec{U}}{\partial s} = \frac{\partial v}{\partial s}\vec{t} + \frac{\partial w}{\partial s}\vec{n} + v\frac{\partial \vec{t}}{\partial s} + w\frac{\partial \vec{n}}{\partial s}$$

Substitution of $\partial\vec{t}/\partial s = -\vec{n}/\rho$ and $\partial\vec{n}/\partial s = \vec{t}/\rho$ converts this to

$$\frac{\partial \vec{U}}{\partial s} = \vec{t}\left(\frac{\partial v}{\partial s} + \frac{w}{\rho}\right) + \vec{n}\left(\frac{\partial w}{\partial s} - \frac{v}{\rho}\right)$$

Transverse strain. - Assuming that $\partial u/\partial s$ is small, where $u(s,z)$ denotes the longitudinal (z-wise) displacements of middle-surface points, the length of the vector $\vec{P'Q'}$ in figure 4 may be taken as the deformed length of the line element PQ. Thus, the transverse strain ε_s at point P is given by

$$\varepsilon_s = \frac{|\vec{P'Q'}| - ds}{ds} \tag{4}$$

But

$$\begin{aligned}\vec{P'Q'} &= \vec{PQ} + \vec{dU} \\ &= \vec{t}\,ds + \frac{\partial \vec{U}}{\partial s}ds \\ &= \left[\vec{t}\left(1 + \frac{\partial v}{\partial s} + \frac{w}{\rho}\right) + \vec{n}\left(\frac{\partial w}{\partial s} - \frac{v}{\rho}\right)\right]ds \end{aligned} \tag{5}$$

Taking the absolute value of this vector, substituting it into equation (4), and assuming small displacements and small displacement gradients, so that terms higher than the first degree in these quantities may be neglected, one obtains

$$\varepsilon_s = \frac{\partial v}{\partial s} + \frac{w}{\rho} \tag{6}$$

At this point, we will make the assumption, as in references 1, 2 and 3, that the middle surface is transversely inextensional, so that ε_s may be equated to zero to obtain the following constraining relation between the w and v displacement components:

$$\frac{\partial v}{\partial s} + \frac{w}{\rho} = 0 \tag{7}$$

This assumption is based on an inference from ring and frame analysis, namely that when flexural deformations can occur, their contribution to the overall deformation usually far exceeds the contribution arising from direct extension, and the latter may therefore be neglected with very little error. It should be noted that the assumption of transverse inextensibility being made here is far less stringent than the assumption of complete middle-surface inextensibility made in previous analysis (e.g., refs. 4, 5 and 6).

In cross sections with smoothly turning tangents (i.e., without corners), w must be a continuous function of s, but ρ may be discontinuous. (For example, in the cross section composed of circular arcs (fig. 1(a)), ρ changes from $+R$ to $-R$ at $s = R\theta$.) Equation (7) therefore implies that $\partial v/\partial s$ will be discontinuous wherever ρ is discontinuous, provided that w does not vanish there.

Rotation. - The rotation in the plane of the cross section of the line segment PQ will be denoted by $\beta(s,z)$, positive if counterclockwise when viewed from the positive end of the z-axis (see fig. 4).

The relationship between the angle of rotation β and the displacement components w and v can be obtained by evaluating the cross product of the vectors $\vec{PQ}$ and $\vec{P'Q'}$ in two ways. First, from the basic definition of the cross product,

$$\vec{PQ} \times \vec{P'Q'} = \vec{k}\ |\vec{PQ}| \cdot |\vec{P'Q'}|\ \sin\beta$$

$$= \vec{k}\ ds \cdot ds \cdot \sin\beta$$

where the inextensibility assumption has been used in replacing $|\vec{P'Q'}|$ by ds. Alternatively, from equations (2) and (5),

$$\vec{PQ} \times \vec{P'Q'} = \vec{k}\ ds \cdot ds \cdot \left(\frac{\partial w}{\partial s} - \frac{v}{\rho}\right)$$

By equating these two expressions one finds that

$$\sin\beta = \frac{\partial w}{\partial s} - \frac{v}{\rho} \tag{8}$$

Assuming that no corners develop as a result of the deformation, $\sin\beta$ must be a continuous function of s. Furthermore, if there are no corners in the undeformed state, the component v must also be a continuous function of s. When equation (8) is viewed in the light of these two statements, it reveals that $\partial w/\partial s$ must be discontinuous wherever ρ is discontinuous (e.g., at the junctions of adjacent circular-arc segments of the cross section) unless v happens to vanish there. The discontinuity in $\partial w/\partial s$ must match the discontinuity in v/ρ in such a way that the right-hand side of equation (8) remains continuous.*

Expressions for v and w in terms of $\sin\beta$ for a region of constant ρ. - For a given cross section, $\sin\beta$ may be regarded as the basic unknown deformation

*The remarks in this paragraph suggest that the continuity condition $\partial w_1/\partial y_1 = \partial w_2/\partial y_2$ used in equation (11) of reference 4 at the junction of the two adjacent circular-arc segments of the cross section may not be appropriate.

function, since the differential equations(7) and (8) can, in principle, be solved simultaneously for w and v in terms of $\sin\beta$. This solution is simple if ρ is constant, as it is in each circular-arc segment of the cross section of main interest (fig. 1(a)). One first eliminates v between equations (7) and (8) to obtain the following differential equation for w for the case ρ = constant:

$$\frac{\partial^2 w}{\partial s^2} + \frac{w}{\rho^2} = \frac{\partial f}{\partial s} \tag{9}$$

where

$$f(s,z) \doteq \sin\beta \tag{10}$$

is a short-hand notation introduced for simplicity. Equation (9) has the solution

$$w = A(z) \sin\frac{s}{\rho} + B(z) \cos\frac{s}{\rho} + g(s,z) \tag{11}$$

where g(s,z) is a particular solution of equation (9) and A and B are arbitrary functions of z. Equations (11) and (8) then give

$$v = A(z) \cos\frac{s}{\rho} - B(z) \sin\frac{s}{\rho} + \rho\left(\frac{\partial g}{\partial s} - f\right) \tag{12}$$

Expressions for v and w for the circular-arc corrugation. - The above results, equations (11) and (12), will now be applied to each segment of the circular-arc corrugation. A typical repeating unit of the cross section of such a corrugation is shown in figure 5. We will designate as Region 1 that circular arc which forms a crest region of the corrugation, and as Region 2 that one which forms a trough or valley. It will be convenient to introduce the auxiliary transverse coordinate $\bar{s}$, measured from the lowest point of the trough (see fig. 5) and related to s as follows:

$$\bar{s} = 2R\theta - s \tag{13}$$

It will also be convenient to introduce auxiliary displacement and rotation parameters $\bar{v}$, $\bar{w}$ and $\bar{\beta}$, which bear the same relationship to $\bar{s}$ as v, w and β bear to s. The definitions and sign convention for $\bar{v}$, $\bar{w}$ and $\bar{\beta}$ are shown in figure 5. The $\bar{v}$, $\bar{w}$ and $\bar{\beta}$ of any point of the cross section are obviously related as follows to the v, w and β of the same point:

$$\bar{v} = -v \tag{14a}$$

$$\bar{w} = -w \tag{14b}$$

$$\bar{\beta} = \beta \tag{14c}$$

Writing equations (11) and (12) first for Region 1, we obtain

$$\begin{aligned} w &= A(z) \sin \frac{s}{R} + B(z) \cos \frac{s}{R} + g(s,z) \\ v &= A(z) \cos \frac{s}{R} - B(z) \sin \frac{s}{R} + R\left(\frac{\partial g}{\partial s} - f\right) \end{aligned} \tag{15}$$

where g(s,z) is now a particular solution of equation (9) with ρ replaced by R; that is, a particular solution of the equation

$$\frac{\partial^2 w}{\partial s^2} + \frac{w}{R^2} = \frac{\partial f}{\partial s} \tag{16}$$

Considering equations (8) and (10) and the symmetry and antisymmetry properties of v and w shown in the lower part of figure 3, it can be concluded that the function f(s,z) is even in s. If we then stipulate that the particular integral g(s,z) be odd in s, the function B(z) may be set equal to zero in equations (15), and these equations become

$$\begin{aligned} w(s,z) &= A(z) \sin \frac{s}{R} + g(s,z) \\ v(s,z) &= A(z) \cos \frac{s}{R} + R\left(\frac{\partial g}{\partial s} - f\right) \end{aligned} \tag{17}$$

From this point on it is to be understood that f(s,z) and g(s,z) are respectively even and odd with respect to s, and that equations (17) apply only in Region 1.

The equations for $\bar{w}$ and $\bar{v}$ for Region 2 are directly analogous to equations (17) and are therefore as follows:

$$\begin{aligned} \bar{w}(\bar{s},z) &= \bar{A}(z)\,\sin\frac{\bar{s}}{R} + \bar{g}(\bar{s},z) \\ \bar{v}(\bar{s},z) &= \bar{A}(z)\,\cos\frac{\bar{s}}{R} + R\left(\frac{\partial\bar{g}}{\partial\bar{s}} - \bar{f}\right) \end{aligned} \tag{18}$$

where $\bar{A}(z)$ is another arbitrary function of z,

$$\begin{aligned} \bar{f}(\bar{s},z) &\equiv \sin\left[\bar{\beta}(\bar{s},z)\right] \\ &= \sin\left[\beta(2R\theta - \bar{s},\, z)\right] \\ &= f(2R\theta - \bar{s},\, z) \end{aligned} \tag{19}$$

and $\bar{g}(\bar{s},z)$ is a particular solution, odd with respect to $\bar{s}$, of the differential equation

$$\frac{\partial^2\bar{w}}{\partial\bar{s}^2} + \frac{\bar{w}}{R^2} = \frac{\partial\bar{f}}{\partial\bar{s}} \tag{20}$$

Equations (10), (13) and (14c) were used in the development of equation (19). Equations (18) are valid only in Region 2.

The continuity requirements on displacement at the junction of Regions 1 and 2 are

$$\begin{aligned} \bar{w}(R\theta,z) &= -\,w(R\theta,z) \\ \bar{v}(R\theta,z) &= -\,v(R\theta,z) \end{aligned} \tag{21a}$$

(Continuity of rotation at such junctions will be insured later on by selecting only continuous functions of s to represent $\beta(s,z)$.) When expressions (17) and (18) are substituted in equations (21a) the latter become

$$\bar{A}(z)\sin\theta + \bar{g}(R\theta,z) = -A(z)\sin\theta - g(R\theta,z)$$

$$\bar{A}(z)\cos\theta + R\left[\left(\frac{\partial\bar{g}}{\partial\bar{s}}\right)_{\bar{s}=R\theta} - \bar{f}(R\theta,z)\right] = -A(z)\cos\theta - R\left[\left(\frac{\partial g}{\partial s}\right)_{s=R\theta} - f(R\theta,z)\right] \tag{21b}$$

which can be rewritten as

$$[\bar{A}(z) + A(z)]\sin\theta = -[\bar{g}(R\theta,z) + g(R\theta,z)] \tag{22}$$

$$[\bar{A}(z) + A(z)]\cos\theta = R\left[2f(R\theta,z) - \left(\frac{\partial\bar{g}}{\partial\bar{s}}\right)_{\bar{s}=R\theta} - \left(\frac{\partial g}{\partial s}\right)_{s=R\theta}\right] \tag{23}$$

The relationship $\bar{f}(R\theta,z) = f(R\theta,z)$, from equation (19), was used in obtaining equation (23).

Equations (22) and (23) are constraining relationships among the functions A, $\bar{A}$, f, g and $\bar{g}$ which must be satisfied to insure the satisfaction of the continuity conditions (21). Either of these equations may be replaced by the following, which is obtained by eliminating $\bar{A}(z) + A(z)$ between the two equations:

$$2f(R\theta,z) = \left(\frac{\partial\bar{g}}{\partial\bar{s}}\right)_{\bar{s}=R\theta} + \left(\frac{\partial g}{\partial s}\right)_{s=R\theta} - [\bar{g}(R\theta,z) + g(R\theta,z)]\frac{\cot\theta}{R} \tag{24}$$

Series Expansions for the Rotations and Displacements in the Plane of the Cross Section

From here on attention will be restricted to the case of the circular-arc corrugation, and expressions will be developed for $\sin\beta \equiv f(s,z)$ and for w, v, $\bar{w}$ and $\bar{v}$ in the form of Fourier series in s.

Series expansion for f(s,z). - The rotation function $\sin\beta \equiv f(s,z)$ will be regarded as the basic unknown defining the deformation of the cross section in its own plane. Inasmuch as the rotation is even in s and periodic over $4R\theta$, an appropriate Fourier series expansion for f(s,z) is

$$f(s,z) = a_o(z) + \sum_{n=1}^{\infty} a_n(z) \cos \frac{n\pi s}{2R\theta} \tag{25}$$

where $a_o(z)$, $a_1(z)$,... are unknown functions of z. This series is postulated for the entire corrugation cross section. With particular reference to figure 5, it applies to the range $-R\theta \leq s \leq 3R\theta$. With equation (25) selected as the form of f(s,z), equation (19) then dictates the following series expansion for $\bar{f}(\bar{s},z)$:

$$\bar{f}(\bar{s},z) = a_o(z) + \sum_{n=1}^{\infty} a_n(z)\ (-1)^n \cos \frac{n\pi \bar{s}}{2R\theta} \tag{26}$$

Determination of $g(s,z)$ and $\bar{g}(\bar{s},z)$. - Expressions for g(s,z) and $\bar{g}(\bar{s},z)$ in series form are obtained by substituting expressions (25) and (26) in the right-hand sides of equations (16) and (20) and then finding the particular integrals of these equations having the desired characteristic of being odd with respect to their first argument. The result of this procedure, when θ is not equal to $\pi/2$, is:

$$\begin{aligned} g(s,z) &= 4R\theta \sum_{n=1}^{\infty} \Lambda_n\, a_n(z) \sin \frac{n\pi s}{2R\theta} \\ \bar{g}(\bar{s},z) &= 4R\theta \sum_{n=1}^{\infty} (-1)^n \Lambda_n\, a_n(z) \sin \frac{n\pi \bar{s}}{2R\theta} \end{aligned} \tag{27}$$

where

$$\Lambda_n \equiv \frac{2n\pi}{(2n\pi)^2 - (4\theta)^2} \tag{28}$$

The n=1 terms of equations (27) are obviously not valid when $\theta = \pi/2$, because Λ_1 (eq. 28)) becomes infinite. It is easily verified that for $\theta = \pi/2$ the particular integrals of equations (16) and 20) corresponding to n=1 become

$$\frac{a_1(z)R}{2}\frac{s}{R}\cos\frac{s}{R} \qquad \text{and} \qquad -\frac{a_1(z)R}{2}\frac{\bar{s}}{R}\cos\frac{\bar{s}}{R}$$

respectively. Thus, for $\theta=\pi/2$ equations (27) must be replaced by the following:

$$\begin{aligned} g(s,z) &= \frac{a_1(z)R}{2}\frac{s}{R}\cos\frac{s}{R} + 4R\theta\sum_{n=2}^{\infty}\Lambda_n\, a_n(z)\sin\frac{n\pi s}{2R\theta} \\ \bar{g}(\bar{s},z) &= -\frac{a_1(z)R}{2}\frac{\bar{s}}{R}\cos\frac{\bar{s}}{R} + 4R\theta\sum_{n=2}^{\infty}(-1)^n\Lambda_n\, a_n(z)\sin\frac{n\pi\bar{s}}{2R\theta} \end{aligned} \tag{27'}$$

Imposition of the continuity constraints. - Substitution of expression (25) and (27) or (27') into the continuity constraint equation (24) yields a relationship among the even-subscripted a_n's. This relationship, when solved for a_o, gives

$$a_o(z) = \sum_{n=2,4,..}^{\infty}(-1)^{n/2}\,\Omega_n\, a_n(z) \tag{29}$$

where

$$\Omega_n \equiv 2n\pi\Lambda_n - 1 \tag{30}$$

Equations (29) and (30) are valid for $\theta = \pi/2$ as well as for all other physically realizable values of θ.

Selecting equation (22) as the second of the two independent continuity constraints, and substituting the appropriate series expansions for g and $\bar{g}$ (eqs. (27') or (27), depending on whether or not $\theta = \pi/2$), one finds that $\bar{A}(z) + A(z) = 0$, whence

$$\bar{A}(z) = -A(z) \tag{31}$$

Displacements. - The displacements in the plane of the cross section are given by equations (17) and (18). Substituting into these equations the series already developed for f, $\bar{f}$, g and $\bar{g}$ (eqs. (25), (26), (27) or (27')), and making

use of equations (29) and (31), one obtains series expressins for w, v, $\bar{w}$ and $\bar{v}$. For the case $\theta \neq \pi/2$, these expressions are

$$w = A(z) \sin \frac{s}{R} + 4R\theta \sum_{n=1}^{\infty} \Lambda_n a_n(z) \sin \frac{n\pi s}{2R\theta}$$

$$v = A(z) \cos \frac{s}{R} + R\left[\sum_{n=1}^{\infty} \Omega_n a_n(z) \cos \frac{n\pi s}{2R\theta} - \sum_{n=2,4,..}^{\infty} (-1)^{n/2} \Omega_n a_n(z)\right] \tag{32}$$

$$\bar{w} = -A(z) \sin \frac{\bar{s}}{R} + 4R\theta \sum_{n=1}^{\infty} (-1)^n \Lambda_n a_n(z) \sin \frac{n\pi \bar{s}}{2R\theta}$$

$$\bar{v} = -A(z) \cos \frac{\bar{s}}{R} + R\left[\sum_{n=1}^{\infty} (-1)^n \Omega_n a_n(z) \cos \frac{n\pi \bar{s}}{2R\theta} - \sum_{n=2,4,..}^{\infty} (-1)^{n/2} \Omega_n a_n(z)\right] \tag{33}$$

For $\theta = \pi/2$ the corresponding expressions are

$$w = A(z) \sin \frac{s}{R} + \frac{a_1(z)R}{2} \frac{s}{R} \cos \frac{s}{R} + 4R\theta \sum_{n=2}^{\infty} \Lambda_n a_n(z) \sin \frac{n\pi s}{2R\theta}$$

$$v = \left[A(z) - \frac{a_1(z)R}{2}\right] \cos \frac{s}{R} - \frac{a_1(z)R}{2} \frac{s}{R} \sin \frac{s}{R} \tag{32'}$$

$$+ R\left[\sum_{n=2}^{\infty} \Omega_n a_n(z) \cos \frac{n\pi s}{2R\theta} - \sum_{n=2,4,..}^{\infty} (-1)^{n/2} \Omega_n a_n(z)\right]$$

$$\bar{w} = -A(z) \sin \frac{\bar{s}}{R} - \frac{a_1(z)R}{2} \frac{\bar{s}}{R} \cos \frac{\bar{s}}{R} + 4R\theta \sum_{n=2}^{\infty} (-1)^n \Lambda_n a_n(z) \sin \frac{n\pi \bar{s}}{2R\theta}$$

$$\bar{v} = \left[-A(z) + \frac{a_1(z)R}{2}\right] \cos \frac{\bar{s}}{R} + \frac{a_1(z)R}{2} \frac{\bar{s}}{R} \sin \frac{\bar{s}}{R} \tag{33'}$$

$$+ R\left[\sum_{n=2}^{\infty} (-1)^n \Omega_n a_n(z) \cos \frac{n\pi \bar{s}}{2R\theta} - \sum_{n=2,4..}^{\infty} (-1)^{n/2} \Omega_n a_n(z)\right]$$

It is to be understood that equations (32) and (32') apply only in Region 1, while (33) and (33') apply only in Region 2.

It is evident from equations (32), (33), (32') and (33') that A(z) represents rigid-body horizontal translations of the cross sections.

Constraints on A(z) and the $a_n(z)$ arising from the end-attachment conditions. - Certain constraints exist on the end values (at z=±b) of w, v, $\bar{w}$ and $\bar{v}$, depending upon which of the four kinds of end attachments (see fig. 2) is present. Some of these constraints are automatically satisfied by the series expressions for w, v, $\bar{w}$ and $\bar{v}$ developed above. Those constraints not automatically satisfied are the following:

For the type (a) end attachments,

$$\bar{v}(0,\pm b) = 0 \tag{34a}$$

For the type (b) end attachments,

$$\bar{v}(0,\pm b) = 0, \qquad v(0,\pm b) = 0 \tag{34b}$$

For the type (c) end attachments,

$$w(R\theta,\pm b) = 0, \qquad v(R\theta,\pm b) = 0 \tag{34c}$$

For the type (d) end attachment

$$\bar{v}(0,\pm b) = 0, \quad v(0,\pm b) = 0, \quad w(R\theta,\pm b) = 0, \quad v(R\theta,\pm b) = 0 \tag{34d}$$

By substituting into equations (34) the series expressions for w, v, $\bar{w}$ and $\bar{v}$, one obtains the following constraining relations for the end values of A(z) and the $a_n(z)$:

For type (a) attachments and $\theta \neq \pi/2$,

$$-A(\pm b) + R\Big[\sum_{n=1}^{\infty} (-1)^n \Omega_n a_n(\pm b) - \sum_{n=2,4,..}^{\infty} (-1)^{n/2} \Omega_n a_n(\pm b)\Big] = 0 \tag{35a.1}$$

For type (a) attachments and $\theta = \pi/2$,

$$-A(\pm b) + \frac{a_1(\pm b)R}{2} + R\Big[\sum_{n=2}^{\infty} (-1)^n \Omega_n a_n(\pm b) - \sum_{n=2,4,..}^{\infty} (-1)^{n/2} \Omega_n a_n(\pm b)\Big] = 0 \tag{35a.2}$$

For type (b) attachments and $\theta \neq \pi/2$ (writing actually the sum and difference of eqs. (34b)),

$$\begin{aligned} &[\Omega_2 a_2 + \Omega_6 a_6 + \Omega_{10} a_{10} + \ldots]_{z=\pm b} = 0 \\ &A(\pm b) + R \sum_{n=1,3,..}^{\infty} \Omega_n a_n(\pm b) = 0 \end{aligned} \tag{35b.1}$$

For type (b) attachments and $\theta = \pi/2$ (again based on the sum and difference of eqs. (34b)),

$$[\Omega_2 a_2 + \Omega_6 a_6 + \Omega_{10} a_{10} + \ldots]_{z=\pm b} = 0$$

$$A(\pm b) - \frac{1}{2} R a_1(\pm b) + R \sum_{n=3,5,..}^{\infty} \Omega_n \, a_n(\pm b) = 0 \tag{35.b2}$$

For type (c) attachments and $\theta \neq \pi/2$,

$$A(\pm b) = 0$$

$$\sum_{n=1,3,..}^{\infty} \Lambda_n (-1)^{\frac{n-1}{2}} a_n(\pm b) = 0 \tag{35c.1}$$

For type (c) attachments and $\theta = \pi/2$,

$$A(\pm b) + 2\pi R \sum_{n=3,5,..}^{\infty} \Lambda_n \, a_n(\pm b) \, (-1)^{\frac{n-1}{2}} = 0$$

$$a_1(\pm b) = 0 \tag{35c.2}$$

For type (d) attachments and $\theta \neq \pi/2$,

Eqs. (35b.1) together with eqs. (35c.1) (35d.1)

For type (d) attachments and $\theta = \pi/2$,

Eqs. (35b.2) together with eqs. (35c.2) (35d.2)

Variational form of the constraints on $A(z)$ and the $a_n(z)$ arising from the end-attachment conditions. - We note for later use that each of equations (35a.1) through (35d.2) has a variational form implying a constraint on the variations $\delta A(\pm b)$ and $\delta a_n(\pm b)$ of the boundary values of $A(z)$ and the $a_n(z)$. For example, the variational form of equation (35a.1) is

$$-\delta A(\pm b) + R\Big[\sum_{n=1}^{\infty} (-1)^n \Omega_n \, \delta a_n(\pm b) - \sum_{n=2,4,..}^{\infty} (-1)^{n/2} \Omega_n \, \delta a_n(\pm b)\Big] = 0$$

This equation and the corresponding ones arising from the rest of equations (35) give rise to the following relationships:

For type (a) attachments and $\theta \neq \pi/2$,

$$\delta A(\pm b) = R\Big[\sum_{n=1}^{\infty} (-1)^n \Omega_n \delta a_n(\pm b) - \sum_{n=2,4,..}^{\infty} (-1)^{n/2} \Omega_n \delta a_n(\pm b)\Big] \tag{36a.1}$$

For type (a) attachments and $\theta = \pi/2$,

$$\delta A(\pm b) = \frac{R\delta a_1(\pm b)}{2} + R\Big[\sum_{n=2}^{\infty} (-1)^n \Omega_n \delta a_n(\pm b) - \sum_{n=2,4,..}^{\infty} (-1)^{n/2} \Omega_n \delta a_n(\pm b)\Big] \tag{36a.2}$$

For type (b) attachments and $\theta \neq \pi/2$,

$$\Omega_2 \delta a_2(\pm b) = -\left[\Omega_6 \delta a_6(\pm b) + \Omega_{10} \delta a_{10}(\pm b) + \ldots\right]$$

$$\delta A(\pm b) = -R \sum_{n=1,3,..}^{\infty} \Omega_n \delta a_n(\pm b) \tag{36b.1}$$

For type (b) attachments and $\theta = \pi/2$,

$$\Omega_2 \delta a_2(\pm b) = -\left[\Omega_6 \delta a_6(\pm b) + \Omega_{10} \delta a_{10}(\pm b) + \ldots\right]$$

$$\delta A(\pm b) = \frac{1}{2} R\delta a_1(\pm b) - R \sum_{n=3,5,..}^{\infty} \Omega_n \delta a_n(\pm b) \tag{36b.2}$$

For type (c) attachments and $\theta \neq \pi/2$,

$$\delta A(\pm b) = 0$$

$$\Lambda_1 \delta a_1(\pm b) = -\sum_{n=3,5,..}^{\infty} \Lambda_n (-1)^{\frac{n-1}{2}} \delta a_n(\pm b) \tag{36c.1}$$

For type (c) attachments and $\theta = \pi/2$,

$$\delta A(\pm b) = -2\pi R \sum_{n=3,5,..}^{\infty} \Lambda_n (-1)^{\frac{n-1}{2}} \delta a_n(\pm b)$$

$$\delta a_1(\pm b) = 0 \tag{36c.2}$$

For type (d) attachments and $\theta \neq \pi/2$,

$$\Omega_2\delta a_2(\pm b) = -\left[\Omega_6\delta a_6(\pm b) + \Omega_{10}\delta a_{10}(\pm b) + \ldots\right]$$

$$\delta A(\pm b) = 0 \tag{36d.1}$$

$$(\Omega_1\Lambda_3 + \Omega_3\Lambda_1)\ \delta a_1(\pm b) = -\sum_{n=5,7,..}^{\infty}\left[\Omega_n\Lambda_3 + \Lambda_n\Omega_3(-1)^{\frac{n-1}{2}}\right]\delta a_n(\pm b)$$

$$(\Omega_1\Lambda_3 + \Omega_3\Lambda_1)\ \delta a_3(\pm b) = -\sum_{n=5,7,..}^{\infty}\left[\Omega_n\Lambda_1 - \Lambda_n\Omega_1(-1)^{\frac{n-1}{2}}\right]\delta a_n(\pm b)$$

For type (d) attachments and $\theta = \pi/2$,

$$\Omega_2\delta a_2(\pm b) = -\left[\Omega_6\delta a_6(\pm b) + \Omega_{10}\delta a_{10}(\pm b) + \ldots\right]$$

$$\delta a_1(\pm b) = 0 \tag{36d.2}$$

$$\delta a_3(\pm b) = \sum_{n=5,7,..}^{\infty} T_n^{(11)}\delta a_n(\pm b)$$

$$\delta A(\pm b) = R\sum_{n=5,7,..}^{\infty} T_n^{(12)}\delta a_n(\pm b)$$

where

$$T_n^{(11)} \equiv -2\left[1 - n(-1)^{\frac{n-1}{2}}\right]/(n^2-1)$$

$$T_n^{(12)} \equiv -\left[3 + n(-1)^{\frac{n-1}{2}}\right]/(4n^2-4) \tag{37}$$

Series Expansions for Longitudinal Displacements

The longitudinal (z-wise) displacements of points on the middle surface will be denoted by $u(s,z)$ and assumed in the form of a term which is linear in s plus a Fourier series in s:

$$u(s,z) = u_o\cdot\frac{s}{2R\theta} + \sum_{n=1}^{\infty} b_n(z)\ \sin\frac{n\pi s}{2R\theta} \tag{38}$$

where $b_n(z)$ are as yet undetermined functions of z, and s is measured from a crest (see fig. 1a or fig. 5). Equation (38) satisfies the requirement that u(s,z) be odd in s. It gives a relative longitudinal displacement of $2u_o$ per corrugation, as required. This can be verified by substituting $s=-2R\theta$ and $s=+2R\theta$ into it. The linear term of equation (38) represents a uniform shear deformation, such as could be obtained by means of continuous attachment of the end cross sections to diaphragms which prevent deformations of the end cross sections in their own planes but offer no resistance to the warping of the end cross sections out of their planer condition. The Fourier series part of equation (38) represents deviations from this uniform shear condition, arising because of the absence of the above-described continuous end attachment.

Equation (38) is valid for both Regions 1 and 2 of figure 5. However, it will be convenient, for later use, to introduce the function $\bar{u}(\bar{s},z)$ to denote the longitudinal (z-wise) displacements of middle-surface points in Region 2. The functions $\bar{u}(\bar{s},z)$ and u(s,z) must have identical values for the same material point; they are therefore related as follows:

$$\bar{u}(\bar{s},z) = u(2R\theta - \bar{s},z)$$

Therefore the series expression for $\bar{u}(\bar{s},z)$ can be obtained by replacing s in equation (38) by $2R\theta - \bar{s}$. The result is

$$\bar{u}(\bar{s},z) = u_o \left(1 - \frac{\bar{s}}{2R\theta}\right) + \sum_{n=1}^{\infty} b_n(z) (-1)^{n+1} \sin \frac{n\pi\bar{s}}{2R\theta} \qquad (38')$$

Constraints on the $b_n(z)$ arising from end-attachment conditions. - Apart from the requirement that the relative longitudinal displacement be

$2u_o$ per corrugation, there are, for attachment conditions (b), (c) and (d) of figure 2, additional requirements due to the presence of attachment points intermediate between A and C. These additional requirements are that in each case attachment point B have a longitudinal displacement that is the mean of the longitudinal displacements of A and C, and in case (d) the attachment point A' have a longitudinal displacement which is the mean of the longitudinal displacements of A and B, while C' similarly have a displacement which is the mean of those of B and C.

Expressed mathematically, these additional requirements are as follows: For type (b) end attachments,

$$u(o,\pm b) = \frac{1}{2}\left[u(-2R\theta,\pm b) + u(2R\theta,\pm b)\right] \tag{i}$$

For type (c) end attachments,

$$u(R\theta,\pm b) = \frac{1}{2}\left[u(-R\theta,\pm b) + u(3R\theta,\pm b)\right] \tag{ii}$$

For type (d) end attachments,

$$u(o,\pm b) = \frac{1}{2}\left[u(-2R\theta,\pm b) + u(2R\theta,\pm b)\right] \tag{iii}$$

$$u(-R\theta,\pm b) = \frac{1}{2}\left[u(-2R\theta,\pm b) + u(o,\pm b)\right] \tag{iv}$$

$$u(R\theta,\pm b) = \frac{1}{2}\left[u(o,\pm b) + u(2R\theta,\pm b)\right] \tag{v}$$

Requirements (i) and (iii) are automatically satisfied by equation (38). However, in order for requirements (ii), (iv) and (v) to be satisfied, the following constraining relation must be imposed on the $b_n(\pm b)$:

$$\sum_{n=1,3,..}^{\infty} b_n(\pm b)\,(-1)^{\frac{n-1}{2}} = 0 \tag{39}$$

In variational form, with the b_1 term separated from the rest, this relation is

$$\delta b_1(\pm b) = -\sum_{n=3,5,..}^{\infty} \delta b_n(\pm b)\ (-1)^{\frac{n-1}{2}} \tag{40}$$

Equations (39) and (40) are needed only for the type (c) and (d) end attachments.

Analysis of Strains

In preparation for the writing of a strain energy expression, expressions will now be developed for the strains at a typical point in the corrugation a distance ζ from the middle surface. Point R in figure 6 represents such a point, and RS is an infinitesimal material fiber through R in the plane of the undeformed cross section and parallel to the middle surface. Its undeformed length is $[1 + (\zeta/\rho)]$ ds, where ds is the length of the corresponding middle-surface fiber PQ. Through point R one can also imagine an infinitesimal fiber segment RT, of length dz, running in the longitudinal direction. (Point T is not shown in figure 6.) Fiber segments RS and RT are at right angles to each other in the undeformed corrugation. During the deformation of the corrugation, points R, S and T move to new positions R', S' and T'. The resulting changes of length of the fibers RS and RT will define the extensional strains of a lamina a distance ζ above the middle surface, and the change of angle between them will define the shear strain of this lamina. In determining positions R', S' and T', the usual assumption will be made that lines, such as PR, normal to the middle surface before deformation are also normal to the middle surface after deformation.

One can start by writing the displacement vector $\vec{V}_P$ of the middle-surface point P. This vector is the vector sum of the displacement in the plane of

the cross section (the vector $\vec{U}$ of fig. 4) and the longitudinal displacement $\vec{k}u$. Thus, utilizing equation (3),

$$\vec{V}_P = \vec{U} + \vec{k}u$$

$$= \vec{t}v + \vec{n}w + \vec{k}u$$

The displacement vector $\vec{V}_R$ of point R will differ from $\vec{V}_P$ by an amount depending on the (assumedly small) rotations of line segment PR, which are β in the plane of the cross section and $\partial w/\partial z$ in the longitudinal plane, in view of the assumption of normal line segments remaining normal. Thus

$$\vec{V}_R = \vec{V}_P - \zeta(\vec{t}\beta + \vec{k}\,\partial w/\partial z)$$

$$= \vec{t}(v - \zeta\beta) + \vec{n}w + \vec{k}(u - \zeta\partial w/\partial z) \tag{41}$$

The displacement vectors $\vec{V}_S$ and $\vec{V}_T$ of points S and T will differ infinitesimally from $\vec{V}_R$ by amounts which depend upon the partial derivatives, with respect to s and z respectively, of the right side of equation (41). Symbolically,

$$\begin{aligned} \vec{V}_S &= \vec{V}_R + (\partial\vec{V}_R/\partial s)\, ds \\ \vec{V}_T &= \vec{V}_R + (\partial V_R/\partial z)\, dz \end{aligned} \tag{42}$$

Evaluating the two partial derivatives of the right side of equation (41) (taking into account the relations $\partial\vec{t}/\partial s = -\vec{n}/\rho$, $\partial\vec{n}/\partial s = \vec{t}/\rho$) and substituting their expressions into equations (42), one obtains

$$\vec{V}_S = \vec{V}_R + \left[\vec{t}\left(\frac{\partial v}{\partial s} - \zeta\,\frac{\partial\beta}{\partial s} + \frac{w}{\rho}\right) + \vec{n}\left(\frac{\partial w}{\partial s} - \frac{v}{\rho} + \beta\,\frac{\zeta}{\rho}\right)\right.$$

$$\left. + \vec{k}\left(\frac{\partial u}{\partial s} - \zeta\,\frac{\partial^2 w}{\partial s\partial z}\right)\right] ds \tag{43}$$

$$\vec{V}_T = \vec{V}_R + \left[\vec{t}\left(\frac{\partial v}{\partial z} - \zeta\,\frac{\partial\beta}{\partial z}\right) + \vec{n}\,\frac{\partial w}{\partial z} + \vec{k}\left(\frac{\partial u}{\partial z} - \zeta\,\frac{\partial^2 w}{\partial z^2}\right)\right] dz$$

It will be convenient to define vectors $\vec{RS}$ and $\vec{RT}$ coinciding with the undeformed fiber segments RS and RT, as well as vectors $\vec{R'S'}$ and $\vec{R'T'}$ coinciding with these fiber segments in their deformed state. The expressions for the first pair of vectors are

$$\begin{aligned} \vec{RS} &= \vec{t}[1 + (\zeta/\rho)]\, ds \\ \vec{RT} &= \vec{k}\, dz \end{aligned} \tag{44}$$

The vector polygon formed by $\vec{RS}$, $\vec{R'S'}$, $\vec{V}_R$ and $\vec{V}_S$ (see fig. 7) readily gives the following expression for $\vec{R'S'}$:

$$\vec{R'S'} = \vec{V}_S - \vec{V}_R + \vec{RS} \tag{45}$$

Similarly,

$$\vec{R'T'} = \vec{V}_T - \vec{V}_R + \vec{RT} \tag{46}$$

Equations (43) and (44) can be used to eliminate $\vec{V}_S - \vec{V}_R$, $\vec{V}_T - \vec{V}_R$, $\vec{RS}$ and $\vec{RT}$ in equations (45) and (46). The resulting right-hand side of equation (45) can then be simplified somewhat through the use of the transverse inextensibility condition, equation (7), and the compatibility condition, equation (8), which for small rotations becomes

$$\frac{\partial w}{\partial s} - \frac{v}{\rho} = \beta$$

In this way the following expressions are obtained for $\vec{R'S'}$ and $\vec{R'T'}$ from equations (45) and (46):

$$\begin{aligned} \vec{R'S'} &= \left[\vec{t}\left(1 + \frac{\zeta}{\rho} - \zeta\,\frac{\partial \beta}{\partial s}\right) + \vec{n}\,\beta\left(1 + \frac{\zeta}{\rho}\right) + \vec{k}\left(\frac{\partial u}{\partial s} - \zeta\,\frac{\partial^2 w}{\partial s \partial z}\right)\right] ds \\ \vec{R'T'} &= \left[\vec{t}\left(\frac{\partial v}{\partial z} - \zeta\,\frac{\partial \beta}{\partial z}\right) + \vec{n}\,\frac{\partial w}{\partial z} + \vec{k}\left(1 + \frac{\partial u}{\partial z} - \zeta\,\frac{\partial^2 w}{\partial z^2}\right)\right] dz \end{aligned} \tag{48}$$

The magnitudes of these two vectors, correct to terms of the first degree in u, v, w and β, are

$$\begin{aligned} |\vec{R'S'}| &= (1 + \frac{\zeta}{\rho} - \zeta \frac{\partial \beta}{\partial s})\, ds \\ |\vec{R'T'}| &= (1 + \frac{\partial u}{\partial z} - \zeta \frac{\partial^2 w}{\partial z^2})\, ds \end{aligned} \tag{49}$$

The transverse strain ε_t, longitudinal strain ε_ℓ, and shear strain γ at point R of the lamina parallel to the middle surface can now be evaluated through the formulas

$$\begin{aligned} \varepsilon_t &= \frac{|\vec{R'S'}| - |\vec{RS}|}{|\vec{RS}|} \\ \varepsilon_\ell &= \frac{|\vec{R'T'}| - |\vec{RT}|}{|\vec{RT}|} \\ \gamma &= \frac{\vec{R'T'} \cdot \vec{R'S'}}{|\vec{R'T'}|\,|\vec{R'S'}|} \end{aligned} \tag{50}$$

Substituting expressions (44), (48) and (49), neglecting terms of higher than the first degree in the deformation quantities, and neglecting ζ/ρ in comparison with unity, one obtains

$$\begin{aligned} \varepsilon_t &= -\zeta \frac{\partial \beta}{\partial s} \\ \varepsilon_\ell &= \frac{\partial u}{\partial z} - \zeta \frac{\partial^2 w}{\partial z^2} \\ \gamma &= \frac{\partial u}{\partial s} + \frac{\partial v}{\partial z} - \zeta(\frac{\partial \beta}{\partial z} + \frac{\partial^2 w}{\partial s \partial z}) \end{aligned} \tag{51}$$

These results are in agreement with equations (2.17) of reference 7.

Stress-Strain Relations

For the sake of generality in these derivations, the material will be assumed to be orthotropic with the following stress-strain relations:

$$\varepsilon_t = \frac{\sigma_t}{E} - \nu'\frac{\sigma_\ell}{E'} \quad , \quad \varepsilon_\ell = \frac{\sigma_\ell}{E'} - \nu\frac{\sigma_t}{E} \quad , \quad \gamma = \frac{\tau}{G} \tag{52a}$$

where σ_t and σ_ℓ and the transverse and longitudinal normal stresses, positive for tension, τ is the shear stress in the s and z directions, E and ν are the Young's modulus and Poisson's ratio associated with uniaxial tension in the transverse direction (the s - direction), E' and ν' the corresponding quantities associated with uniaxial tension in the longitudinal direction (the z-direction), and G is the shear modulus associated with τ. In inverted form, equations (52a) are

$$\sigma_t = \frac{E}{1-\nu\nu'}(\varepsilon_t + \nu'\varepsilon_\ell) \quad , \quad \sigma_\ell = \frac{E'}{1-\nu\nu'}(\varepsilon_\ell + \nu\varepsilon_t), \quad \tau = G\gamma \tag{52b}$$

It will be assumed that a strain energy density exists, and therefore that

$$\nu E' = \nu' E \tag{53}$$

Eliminating the strains in equations (52b) by use of equations (51), one obtains the following stress-displacement relations:

$$\begin{aligned}
\sigma_t &= \frac{E}{1-\nu\nu'}\left[-\zeta\frac{\partial\beta}{\partial s} + \nu'\left(\frac{\partial u}{\partial z} - \zeta\frac{\partial^2 w}{\partial z^2}\right)\right] \\
\sigma_\ell &= \frac{E'}{1-\nu\nu'}\left[\frac{\partial u}{\partial z} - \zeta\frac{\partial^2 w}{\partial z^2} - \nu\zeta\frac{\partial\beta}{\partial s}\right] \\
\tau &= G\left(\frac{\partial u}{\partial s} + \frac{\partial v}{\partial z}\right) - G'\zeta\left(\frac{\partial\beta}{\partial z} + \frac{\partial^2 w}{\partial s\partial z}\right)
\end{aligned} \tag{54}$$

where G' has the same meaning as G, the prime mark being merely a tracer to distinguish those contributions in the strain energy expression (presently

to be developed) due to torsional shear stress from those due to middle-surface shear stress.

Strain Energy Expression

The strain energy of an infinitesimal rectangular parallelepiped of material of thickness $d\zeta$, length dz, and width $[1 + (\zeta/\rho)]ds$ is

$$(dU)_1 = \frac{1}{2}(\sigma_t \varepsilon_t + \sigma_\ell \varepsilon_\ell + \tau\gamma)\ (1 + \frac{\zeta}{\rho})\ d\zeta\ ds\ dz \tag{55}$$

Neglecting ζ/ρ in comparison with 1, substituting expressions (54) for the stresses and (51) for the strains, and integrating through the thickness, from $\zeta = -t/2$ to $\zeta = +t/2$, one arrives at the following strain energy associated with the element $ds\ dz$ of the middle surface:

$$(dU)_2 = \frac{1}{2}\Big[E_z t\Big(\frac{\partial u}{\partial z}\Big)^2 + Gt\Big(\frac{\partial u}{\partial s} + \frac{\partial v}{\partial z}\Big)^2 + D_s \frac{\partial \beta}{\partial s}\Big(\frac{\partial \beta}{\partial s} + \nu' \frac{\partial^2 w}{\partial z^2}\Big)$$

$$+ D_z \frac{\partial^2 w}{\partial z^2}\Big(\frac{\partial^2 w}{\partial z^2} + \nu \frac{\partial \beta}{\partial s}\Big) + D_{sz}\Big(\frac{\partial \beta}{\partial z} + \frac{\partial^2 w}{\partial s \partial z}\Big)^2\Big]\ ds\ dz \tag{56}$$

where

$$E_z \equiv \frac{E'}{1-\nu\nu'}\ ,\quad D_z \equiv \frac{E't^3}{12(1-\nu\nu')}\ ,\quad D_s \equiv \frac{Et^3}{12(1-\nu\nu')},\ D_{sz} \equiv \frac{G't^3}{12} \tag{57}$$

Equation (56) applies to both Regions 1 and 2 of figure 5. However, another form of $(dU)_2$ especially suitable for Region 2 can be obtained by merely replacing s, u, v, w and β everywhere in equation (56) by $\bar{s}$, $\bar{u}$, $\bar{v}$, $\bar{w}$ and $\bar{\beta}$ respectively.

By integrating equation (56), and its counterpart for Region 2, with respect to z from -b to +b, and with respect to s and $\bar{s}$ from $-R\theta$ to $R\theta$, one can obtain the strain energy of an entire corrugation. Considering the symmetry properties of the displacements, it is evidently sufficient to integrate over half a corrugation (i.e., from s = 0 to $R\theta$ and $\bar{s}$ = 0 to $R\theta$) and multiply the results by 2. The following expression is thus obtained for the strain energy U of a single corrugation:

$$U = \int_{-b}^{b} \int_{o}^{R\theta} \left[E_z t \left(\frac{\partial u}{\partial z}\right)^2 + Gt \left(\frac{\partial u}{\partial s} + \frac{\partial v}{\partial z}\right)^2 + D_s \frac{\partial \beta}{\partial s} \left(\frac{\partial \beta}{\partial s} + \nu' \frac{\partial^2 w}{\partial z^2}\right) \right.$$

$$\left. + D_z \frac{\partial^2 w}{\partial z^2} \left(\frac{\partial^2 w}{\partial z^2} + \nu \frac{\partial \beta}{\partial s}\right) + D_{sz} \left(\frac{\partial \beta}{\partial z} + \frac{\partial^2 w}{\partial s \partial z}\right)^2 \right] ds\, dz$$

$$+ \int_{-b}^{b} \int_{o}^{R\theta} \left[E_z t \left(\frac{\partial \bar{u}}{\partial z}\right)^2 + Gt \left(\frac{\partial \bar{u}}{\partial \bar{s}} + \frac{\partial v}{\partial z}\right)^2 + D_s \frac{\partial \bar{\beta}}{\partial \bar{s}} \left(\frac{\partial \bar{\beta}}{\partial \bar{s}} + \nu' \frac{\partial^2 \bar{w}}{\partial z^2}\right) \right.$$

$$\left. + D_z \frac{\partial^2 \bar{w}}{\partial z^2} \left(\frac{\partial^2 \bar{w}}{\partial z^2} + \nu \frac{\partial \bar{\beta}}{\partial \bar{s}} + D_{sz} \left(\frac{\partial \bar{\beta}}{\partial z} + \frac{\partial^2 \bar{w}}{\partial \bar{s} \partial z}\right)^2 \right] d\bar{s}\, dz \qquad (58)$$

The following series can now be substituted for the deformation quantities appearing in equation (58):

For β: Eq. (25)

For $\bar{\beta}$: Eq. (26)

For u: Eq. (38)

For $\bar{u}$: Eq. (38')

For w and v: Eqs. (32) if $\theta \neq \pi/2$; eqs. (32') if $\theta = \pi/2$

For $\bar{w}$ and $\bar{v}$: Eqs. (33) if $\theta \neq \pi/2$; eqs. (33') if $\theta = \pi/2$

If these substitutions are made, the integrations with respect to s and $\bar{s}$ carried out, and a_o eliminated through equation (29), one obtains the following strain energy of a single corrugation for the case $\theta \neq \pi/2$:

$$U = \int_{-b}^{b} \Big\{ E_z t R\theta \sum (b_n')^2 + GtR\Big[\frac{1}{2\theta} \Big(\frac{u_o}{R}\Big)^2 + 2\theta \Big(\sum_{n \text{ even}} T_n^{(1)} a_n' R\Big)^2$$

$$+ S^{(1)} \frac{u_o}{R} A' + \frac{u_o}{R} \sum_{n \text{ odd}} T_n^{(2)} a_n' R - 4\Big(\sum_{n \text{ even}} T_n^{(1)} a_n' R\Big) \sum_{n \text{ odd}} \frac{b_n}{R} (-1)^{\frac{n-1}{2}}$$

$$+ S^{(2)} (A')^2 + A' \sum_{n \text{ even}} \frac{b_n}{R} T_n^{(3)} + A' \sum_{n \text{ odd}} a_n' R \, T_n^{(4)}$$

$$+ \frac{\pi^2}{4\theta} \sum n^2 \Big(\frac{b_n}{R}\Big)^2 + \theta \sum (\Omega_n a_n' R)^2 + \sum_{m+n \text{ odd}} \sum S_{mn} \frac{b_n}{R} (a_m' R)\Big]$$

$$+ \frac{D_s}{R} \frac{\pi^2}{4\theta} \sum n^2 a_n^2 + \frac{D_s \nu' + D_z \upsilon}{R} \Big[-A'' R \sum_{n \text{ odd}} T_n^{(5)} a_n - \sum T_n^{(6)} a_n (a_n'' R^2)\Big]$$

$$+ \frac{D_z}{R} \Big[S^{(3)} (A'' R)^2 + A'' R \sum_{n \text{ odd}} T_n^{(7)} a_n'' R^2 + \sum T_n^{(8)} (a_n'' R^2)^2\Big]$$

$$+ \frac{D_{sz}}{R} \Big[2\theta \Big(\sum_{n \text{ even}} T_n^{(1)} a_n' R\Big)^2 + S^{(2)} (A')^2 + A' \sum_{n \text{ odd}} T_n^{(9)} a_n' R$$

$$+ \sum T_n^{(10)} (a_n' R)^2\Big]\Big\} dz \tag{59}$$

where

$$(\,)' \equiv \frac{\partial (\,)}{\partial z} \quad , \quad (\,)'' \equiv \frac{\partial^2 (\,)}{\partial z^2}$$

$$S^{(1)} \equiv \frac{2\sin\theta}{\theta} \quad , \quad S^{(2)} \equiv \theta + \frac{1}{2} \sin 2\theta, \quad S^{(3)} \equiv \theta - \frac{1}{2} \sin 2\theta \tag{60}$$

$$S_{mn} \equiv \frac{2n}{\left(\frac{m\pi}{2\theta}\right)^2 - 1} \left[\frac{(-1)^{\frac{m-n-1}{2}}}{m-n} + \frac{(-1)^{\frac{m+n-1}{2}}}{m+n} \right] \tag{61}$$

$$T_n^{(1)} \equiv \Omega_n (-1)^{n/2}$$

$$T_n^{(2)} \equiv \frac{4}{n\pi} (-1)^{\frac{n-1}{2}} \Omega_n$$

$$T_n^{(3)} \equiv \frac{-2n\pi}{\theta} (-1)^{n/2} \Omega_n \sin\theta$$

$$T_n^{(4)} \equiv \frac{2n\pi}{\theta} (-1)^{\frac{n-1}{2}} \Omega_n^2 \cos\theta \tag{62}$$

$$T_n^{(5)} \equiv \frac{n\pi}{\theta} (-1)^{\frac{n-1}{2}} \Omega_n \cos\theta$$

(equations continued on next page)

$$T_n^{(6)} \equiv \frac{n^2\pi^2}{4\theta}\,\Omega_n$$

$$T_n^{(7)} \equiv T_n^{(4)}$$

$$T_n^{(8)} \equiv \frac{n^2\pi^2}{4\theta}\,\Omega_n^2$$

$$T_n^{(9)} \equiv \left[2\left(\frac{n\pi}{2\theta}\right)^2 - 1\right]T_n^{(4)}$$

$$T_n^{(10)} \equiv \theta\left[2\left(\frac{n\pi}{2\theta}\right)^2 - 1\right]^2\Omega_n^2$$

and the following interpretations are to be understood for the summation symbols: Where a summation sign appears with no qualifying notation beneath it, the summation is over the range $n=1,2,3,\ldots,\infty$. The notation "n odd" underneath a summation sign means that the summation is over $n=1,3,5\ldots,\infty$; and the notation "n even" means summation over $n=2,4,6,\ldots,\infty$. The double summation, with the notation "m+n odd," covers only those combinations of positive integral values of m and n for which m+n is odd (e.g., m=1, n=2,4,6,...; m=2, n=1,3,5,...; etc.).

An equation similar to (59) is obtained for the special case, $\theta = \pi/2$. However, for the sake of brevity, this expression will not be given, and the remainder of the derivations will apply only to the general case, $\theta \neq \pi/2$.

Total Potential Energy and its First Variation*

The total potential energy (TPE) of a single corrugation (AC in fig. 2) consists of the strain energy U plus the potential energy of any prescribed loads. Regarding the resultant shear forces F along the sides (A and C) of

*From this point on, the analysis is restricted to the case $\theta \neq \pi/2$

the corrugation to be prescribed (rather than the relative shearing displacement $2u_o$), and considering the fact that these forces are acting on inextensible generators, their potential energy is seen to be $-F\cdot 2u_o$. The total potential energy of the single corrugations is therefore

$$TPE = -F\cdot 2u_o + U \tag{63}$$

where U is given by equation (59) when $\theta \neq \pi/2$, F is regarded as given, and u_o is now regarded as an unknown deformation constant resulting from the application of F.

The TPE, equation (63), is a functional of u_o, $A(z)$, $a_1(z)$, $a_2(z)\ldots$, $b_1(z)$, $b_2(z),\ldots$. In accordance with the method of minimum total potential energy, we seek that value of u_o and those forms of $A(z)$, $a_1(z)$, etc. which will make the TPE stationary with respect to all small variations in u_o, $A(z)$, $a_1(z)$, etc.

The first variation of the TPE, obtained by means of the standard technique of variational calculus, is

$$\begin{aligned}
\delta(TPE) = -2F\cdot\delta u_o + \int_{-b}^{b} \Bigg\{ & 2E_z tR\theta \sum b_n'(\delta b_n)' \\
& + GtR\Bigg\{\frac{1}{\theta}\frac{u_o}{R}\frac{\delta u_o}{R} + 4\theta\Big[\sum_{n\ \text{even}} T_n^{(1)} a_n' R\Big]\Big[\sum_{m\ \text{even}} T_m^{(1)}(\delta a_m R)'\Big] \\
& + S^{(1)}\Big[\frac{u_o}{R}(\delta A)' + A'\frac{\delta u_o}{R}\Big] + \frac{\delta u_o}{R}\sum_{n\ \text{odd}} T_n^{(2)} a_n' R \\
& + \frac{u_o}{R}\sum_{n\ \text{odd}} T_n^{(2)}(\delta a_n R)' - 4\Big[\sum_{n\ \text{even}} T_n^{(1)} a_n' R\Big]\Big[\sum_{m\ \text{odd}} \frac{\delta b_m}{R}(-1)^{\frac{m-1}{2}}\Big] \\
& - 4\Big[\sum_{n\ \text{odd}} \frac{b_n}{R}(-1)^{\frac{n-1}{2}}\Big]\Big[\sum_{m\ \text{even}} T_m^{(1)}(\delta a_m R)'\Big] + 2S^{(2)}A'(\delta A)' \\
& + (\delta A)'\sum_{n\ \text{even}} \frac{b_n}{R} T_n^{(3)} + A'\sum_{n\ \text{even}} \frac{\delta b_n}{R} T_n^{(3)} + (\delta A)'\sum_{n\ \text{odd}} a_n' R\, T_n^{(4)}
\end{aligned}$$

(equation continued on next page)

$$+ A' \sum_{n\ \mathrm{odd}} (\delta a_n R)' \, T_n^{(4)} + \frac{\pi^2}{2\theta} \sum n^2 \frac{b_n}{R} \frac{\delta b_n}{R}$$

$$+ 2\theta \sum \Omega_n^2 \, a_n' R \, (\delta a_n R)' + \sum_{m \neq n} \sum_{\mathrm{odd}} S_{mn} \left[\frac{b_n}{R} (\delta a_m R)' + a_m' R \frac{\delta b_n}{R} \right] \Bigg\}$$

$$+ \frac{D_s}{R} \frac{\pi^2}{2\theta} \sum n^2 a_n \delta a_n + \frac{D_s \nu' + D_z \nu}{R} \Bigg\{ - A'' R \sum_{n\ \mathrm{odd}} T_n^{(5)} \delta a_n - (\delta A \cdot R)'' \sum_{n\ \mathrm{odd}} T_n^{(5)} a_n$$

$$- \sum T_n^{(6)} \left[a_n'' R^2 \delta a_n + a_n (\delta a_n R^2)'' \right] \Bigg\}$$

$$+ \frac{D_z}{R} \Bigg\{ 2 \, S^{(3)} A'' R (\delta A \cdot R)'' + A'' R \sum_{n\ \mathrm{odd}} T_n^{(7)} (\delta a_n R^2)''$$

$$+ (\delta A \cdot R)'' \sum_{n\ \mathrm{odd}} T_n^{(7)} a_n'' R^2 + 2 \sum T_n^{(8)} a_n'' R^2 (\delta a_n R^2)'' \Bigg\}$$

$$+ \frac{D_{sz}}{R} \Bigg\{ 4\theta \left[\sum_{n\ \mathrm{even}} T_n^{(1)} a_n' R \right] \left[\sum_{m\ \mathrm{even}} T_m^{(1)} (\delta a_m R)' \right] + 2 S^{(2)} A' (\delta A)'$$

$$+ A' \sum_{n\ \mathrm{odd}} T_n^{(9)} (\delta a_n R)' + (\delta A)' \sum_{n\ \mathrm{odd}} T_n^{(9)} a_n' R$$

$$+ 2 \sum T_n^{(10)} a_n' R \, (\delta a_n R)' \Bigg\} \Bigg\} dz \qquad (64)$$

Any term in equation (64) which involves derivatives of variations can be integrated by parts a sufficient number of times so that the resulting integrands will involve only the variations themselves, not the derivatives of the variations. For example,

$$\int_{-b}^{b} b_n' \, (\delta b_n)' \, dz = b_n' \, (\delta b_n) \Big|_{-b}^{b} - \int_{-b}^{b} b_n'' (\delta b_n) \, dz$$

Applying this technique and some straightforward simplifications, one can reduce equation (64) to the following form:

$$\delta(TPE) \equiv \delta u_o \cdot Gtu_o \cdot I + \int_{-b}^{b} \frac{\delta A}{R^2} \cdot L_A \, dz$$

$$+ \int_{-b}^{b} \sum_{m=1}^{\infty} \frac{\delta a_m}{R} \cdot L_{a_m} \, dz + \int_{-b}^{b} \sum_{m=1}^{\infty} \delta b_m \cdot L_{b_m} \, dz$$

$$+ \left(\frac{\delta A}{R} \cdot B_A\right) \Big|_{-b}^{b} + \left[(\delta A)' \cdot B_{A'}\right] \Big|_{-b}^{b}$$

$$+ \sum_{m=1}^{\infty} \left[(\delta a_m) \cdot B_{a_m}\right] \Big|_{-b}^{b} + \sum_{m=1}^{\infty} \left[R(\delta a_m)' \cdot B_{a_m'}\right] \Big|_{-b}^{b}$$

$$+ 2E_z tR\theta \sum_{m=1}^{\infty} \left[(\delta b_m)\, b_m'\right] \Big|_{-b}^{b} \tag{65}$$

where

$$I \equiv -\frac{2F}{Gtu_o} + \frac{2b}{R\theta} + S^{(1)} \frac{A}{u_o} \Big|_{-b}^{b} + \sum_{n\ \text{odd}} T_n^{(2)} \frac{a_n R}{u_o} \Big|_{-b}^{b} \tag{66}$$

$$L_A \equiv GtR^2(-2S^{(2)}A''R - \sum_{n\ \text{even}} T_n^{(3)} b_n' - \sum_{n\ \text{odd}} T_n^{(4)} a_n'' R^2)$$

$$+ D_{sz}\,(-2S^{(2)}A''R - \sum_{n\ \text{odd}} T_n^{(9)} a_n'' R^2)$$

$$+ D_z\,(2S^{(3)}A''''R^3 + \sum_{n\ \text{odd}} T_n^{(7)} a_n'''' R^4)$$

$$- (D_s\nu' + D_z\nu) \sum_{n\ \text{odd}} T_n^{(5)} a_n'' R^2 \tag{67}$$

$$L_{a_m} \equiv GtR^2(-\Delta_{m1}\, T_m^{(4)} A''R - 4\theta\, \Delta_{m2}\, T_m^{(1)} \sum_{n\ \text{even}} T_n^{(1)} a_n'' R^2$$

$$-2\theta\Omega_m^2 a_m'' R^2 + 4\Delta_{m2} T_m^{(1)} \sum_{n\ \text{odd}} (-1)^{\frac{n-1}{2}} b_n' - \sum_{\substack{n+m \\ \text{odd}}} S_{mn}\, b_n')$$

$$+ D_s\left(\frac{\pi^2}{2\theta}\, m^2 a_m\right) + D_{sz}\,(-\Delta_{m1}\, T_m^{(9)} A''R$$

$$- 4\theta\, \Delta_{m2}\, T_m^{(1)} \sum_{n\ \text{even}} T_n^{(1)} a_n'' R^2 - 2T_m^{(10)} a_m'' R^2)$$

$$+ D_z(\Delta_{m1}\, T_m^{(7)} A''''R^3 + 2\, T_m^{(8)} a_m'''' R^4)$$

$$- (D_s\nu' + D_z\nu)\,(\Delta_{m1}\, T_m^{(5)} A''R + 2\, T_m^{(6)} a_m'' R^2) \tag{68}$$

$$L_{b_m} = -2\,E_z t\theta b_m'' R + Gt(\Delta_{m2} T_m^{(3)} A'$$

$$- 4\,\Delta_{m1}(-1)^{\frac{m-1}{2}} \sum_{n\ even} T_n^{(1)} a_n' R + \sum_{n+m\ odd} S_{nm} a_n' R$$

$$+ \frac{\pi^2}{2\theta} m^2 \frac{b_m}{R}) \tag{69}$$

$$B_A \equiv GtR^2(S^{(1)} \frac{u_o}{R} + 2S^{(2)} A' + \sum_{n\ odd} T_n^{(4)} a_n' R + \sum_{n\ even} T_n^{(3)} \frac{b_n}{R})$$

$$+ D_{sz}(\sum_{n\ odd} T_n^{(9)} a_n' R + 2S^{(2)} A')$$

$$- D_z(2S^{(3)} A''' R^2 + \sum_{n\ odd} T_n^{(7)} a_n''' R^3)$$

$$+ (D_s \nu' + D_z \nu) \sum_{n\ odd} T_n^{(5)} a_n' R \tag{70}$$

$$B_{A'} \equiv D_z(2S^{(3)} A'' R + \sum_{n\ odd} T_n^{(7)} a_n'' R^2) - (D_s \nu' + D_z \nu) \sum_{n\ odd} T_n^{(5)} a_n \tag{71}$$

$$B_{a_m} \equiv GtR^2(\Delta_{m1} T_m^{(2)} \frac{u_o}{R} + \Delta_{m1} T_m^{(4)} A' + 4\theta\,\Delta_{m2} T_m^{(1)} \sum_{n\ even} T_n^{(1)} a_n' R$$

$$+ 2\theta\Omega_m^2 a_m' R - 4\,\Delta_{m2} T_m^{(1)} \sum_{n\ odd} (-1)^{\frac{n-1}{2}} \frac{b_n}{R}$$

$$+ \sum_{n+m\ odd} S_{mn} \frac{b_n}{R})$$

$$+ D_{sz}(\Delta_{m1} T_m^{(9)} A' + 4\theta\Delta_{m2} T_m^{(1)} \sum_{n\ even} T_n^{(1)} a_n' R + 2T_m^{(10)} a_m' R)$$

$$- D_z(\Delta_{m1} T_m^{(7)} A''' R^2 + 2T_m^{(8)} a_m''' R^3)$$

$$+ (D_s \nu' + D_z \nu)\, T_m^{(6)} a_m' R \tag{72}$$

$$B_{a_m'} \equiv D_z(\Delta_{m1} T_m^{(7)} A'' R + 2T_m^{(8)} a_m'' R^2) - (D_s \nu' + D_z \nu)\, T_m^{(6)} a_m \tag{73}$$

with

$$\Delta_{m1} \equiv \begin{cases} 1 \text{ if } m \text{ is odd} \\ 0 \text{ if } m \text{ is even} \end{cases}$$

$$\Delta_{m2} \equiv \begin{cases} 0 \text{ if } m \text{ is odd} \\ 1 \text{ if } m \text{ is even} \end{cases} \tag{74}$$

$$( )''' \equiv \partial^3( )/\partial z^3$$

$$( )'''' \equiv \partial^4( )/\partial z^4$$

The boundary terms (B.T.) in equation (65) (i.e., those with the symbol $\Big|_{-b}^{b}$) contain variations which are not completely independent of one another because of the constraints, equations (36) and (40), arising from the end-attachment conditions. Using equations (36) and (40) to eliminate the variations which appear on the left-hand sides of these equations, one reduces the boundary terms (B.T.) of equation (65) to forms in which the variations are entirely independent of each other. For the case $\theta \neq \pi/2$, these forms are as follows:

For type (a) end attachments,

$$\begin{aligned} \text{B.T.} = \{ & (\delta A)' B_{A'} + R \sum_m (\delta a_m)' B_{a_m'} + 2E_z t R\theta \sum_m (\delta b_m) b_m' \\ & + \sum_{m \text{ odd}} (\delta a_m) (B_{a_m} - \Omega_m B_A) \\ & + \sum_{m \text{ even}} (\delta a_m) [B_{a_m} + \Omega_m B_A \{1-(-1)^{m/2}\}] \}\Big|_{-b}^{b} \end{aligned} \tag{75}$$

For type (b) end attachments,

$$\begin{aligned} \text{B.T.} = [& (\delta A)' B_{A'} + R \sum_m (\delta a_m)' B_{a_m'} + 2E_z t R\theta \sum_m (\delta b_m) b_m' + \sum_{m \text{ odd}} (\delta a_m)(B_{a_m} - \Omega_m B_A) \\ & + (\delta a_4) B_{a_4} + (\delta a_8) B_{a_8} + (\delta a_{12}) B_{a_{12}} + \ldots \\ & + (\delta a_6) \left(B_{a_6} - \frac{\Omega_6}{\Omega_2}\right) + (\delta a_{10}) \left(B_{a_{10}} - \frac{\Omega_{10}}{\Omega_2}\right) + \ldots] \Big|_{-b}^{b} \end{aligned} \tag{76}$$

For type (c) end attachments,

$$\text{B.T.} = \{(\delta A)' B_{A'} + R \sum_m (\delta a_m)' B_{a_m'} + 2E_z tR\theta\Big[\sum_{m\ \text{even}} (\delta b_m) b_m' + \sum_{m=3,5,..}^{\infty} (\delta b_m) \{b_m' - (-1)^{\frac{m-1}{2}} b_1'\}\Big] + \sum_{m\ \text{even}} (\delta a_m) B_{a_m} + \sum_{m=3,5,..}^{\infty} (\delta a_m) \Big[B_{a_m} - B_{a_1} \frac{\Lambda_m}{\Lambda_1} (-1)^{\frac{m-1}{2}}\Big]\} \Big|_{-b}^{b} \tag{77}$$

For type (d) end attachments,

$$\begin{aligned}\text{B.T.} = \{&(\delta A)' B_{A'} + R \sum_m (\delta a_m)' B_{a_m'} \\ &+ 2E_z tR\theta\Big[\sum_{m\ \text{even}} (\delta b_m) b_m' + \sum_{m=3,5,..}^{\infty} (\delta b_m)\{b_m' - (-1)^{\frac{m-1}{2}} b_1'\}\Big] \\ &+ (\delta a_4) B_{a_4} + (\delta a_8) B_{a_8} + (\delta a_{12}) B_{a_{12}} + \cdots \\ &+ (\delta a_6)\Big(B_{a_6} - \frac{\Omega_6}{\Omega_2}\Big) + (\delta a_{10})\Big(B_{a_{10}} - \frac{\Omega_{10}}{\Omega_2}\Big) + \cdots + \sum_{m=5,7,..}^{\infty} (\delta a_m) T_m^{(13)}\Big\}\Big|_{-b}^{b}\end{aligned} \tag{78}$$

where

$$T_m^{(13)} \equiv B_{a_m} - \frac{B_{a_1}[\Omega_m\Lambda_3 + \Lambda_m\Omega_3(-1)^{\frac{m-1}{2}}] + B_{a_3}[\Omega_m\Lambda_1 - \Lambda_m\Omega_1(-1)^{\frac{m-1}{2}}]}{\Omega_1\Lambda_3 + \Omega_3\Lambda_1} \tag{79}$$

It is to be understood, from this point on, that the boundary terms in equation (65) are considered to be replaced by the appropriate one of the above B.T. expressions, depending on the type of end attachments.

Differential Equations and Boundary Conditions

In accordance with the method of minimum total potential energy, the best u_o, $A(z)$, $a_n(z)$ and $b_n(z)$ for a given F are taken to be those which minimize the TPE; i.e., those which make the δ(TPE) (eq.(65) with the boundary

terms replaced by the appropriate B.T. expression from Eqs. (75) through (78)) vanish. The vanishing of the first term and the integrals in the right-hand side of equation (65) necessitates the following conditions on u_o, A(z), the $a_m(z)$, and the $b_m(z)$:

$$I = 0 \tag{80}$$

$$\left.\begin{aligned} L_A &= 0 \\ L_{a_m} &= 0 \qquad \text{for } m = 1, 2, 3,\ldots \\ L_{b_m} &= 0 \qquad \text{for } m = 1, 2, 3,\ldots \end{aligned}\right\} \tag{81}$$

(Equation (80) is an algebraic equation, while equations (81) are differential equations.) The vanishing of the boundary terms (i.e., the vanishing of the appropriate B.T. expression from eqs. (75) through (78)) leads to the so-called natural boundary conditions on the $a_m(z)$, the $b_m(z)$ and A(z). For example, for the type (a) end attachments, the vanishing of expression (75) leads to the following conditions to be satisfied at $z=\pm b$:

$$\begin{aligned} B_{A'} &= 0 \\ B_{a_m'} &= 0 \qquad \text{for } m = 1, 2, 3,\ldots \\ b_m' &= 0 \qquad \text{for } m = 1, 2, 3,\ldots \\ B_{a_m} - \Omega_m B_A &= 0 \qquad \text{for } m = 1, 3, 5,\ldots \\ B_{a_m} + \Omega_m B_A\{1-(-1)^{m/2}\} &= 0 \quad \text{for } m = 2, 4, 6,\ldots \end{aligned} \tag{82}$$

The corresponding natural boundary conditions for the other types of end attachments can easily be discerned from equations (76) through (78).

In addition to the natural boundary conditions discussed above, there are also the geometric boundary conditions, equations (35) and (39), to be satisfied.

The differential equations (81) and the boundary conditions (82), (35) and (39) permit A(z), the $a_m(z)$, and the $b_m(z)$ to be solved for in terms of u_o. Equation (80) will then give u_o in terms of F (i.e., essentially the stiffness).

Inasmuch as equations (81) constitute an infinitely large system, they can be solved only in an approximate sense. This is done by assuming that all the a_n of equation (25) for n greater than a specific integer M, and all the b_n of equation (38) for n greater than a specific integer N, are identically zero. This reduces the infinite system (81) to a finite system, which consists of linear differential equations with constant coefficients, whose solution can in principle be obtained by standard techniques. Improvements in the solution are effected by increasing M and N until no further significant changes are observed in the main numerical results, namely the stiffness furnished by equation (80) and the flexural strains furnished by the first of equations (51).

An examination of the definitions of L_A, L_{a_m}, and L_{b_m} (eqs. (67)-(69)) shows that the system of differential equations (81) can be split into the following two sub-systems containing different sets of unknowns:

$$\left.\begin{aligned} L_A &= 0 \\ L_{a_m} &= 0 \qquad \text{for } m = 1, 3, 5,\ldots \\ L_{b_m} &= 0 \qquad \text{for } m = 2, 4, 6,\ldots \end{aligned}\right\} \quad (83a)$$

$$\left.\begin{aligned} L_{a_m} &= 0 \qquad \text{for } m = 2, 4, 6,\ldots \\ L_{b_m} &= 0 \qquad \text{for } m = 1, 3, 5,\ldots \end{aligned}\right\} \quad (83b)$$

The sub-system (83a) involves only A(z), the $a_m(z)$ with m odd, and the $b_m(z)$ with m even, while sub-system (83b) involves the remaining unknowns, namely the $a_m(z)$ with m even and the $b_m(z)$ with m odd. This splitting is a very fortunate circumstance; without it the solution of equations (81) would require much more work.

It should be noted that although the two groups of unknowns are uncoupled in the differential equations, they are not completely uncoupled, for they are brought together again in the boundary conditions.

Simplification of differential equations and boundary conditions. - The contributions to the strain energy (eq. (58)) arising from the longitudinal curvatures $\partial^2 w/\partial z^2$ and $\partial^2 \bar{w}/\partial z^2$ can be expected to be small compared to those arising from some of the other terms. If these contributions are neglected, a considerable simplification, including a lowering of the order, results in the differential equations and boundary conditions. The neglect of the longitudinal curvature terms can be effected by setting D_z and ν' both equal to zero in the strain energy expression (eq. (58)) and all subsequent equations.

Alternate Solution, Based on Algebraic Equations

In the foregoing, the requirement of the vanishing of the δ(TPE), equation (65), was used as a basis for obtaining the differential equations and some of the boundary conditions governing A(z), the $a_m(z)$, and the $b_m(z)$.

An alternate procedure is possible which leads to algebraic rather than differential equations. In this alternate procedure one expands the unknown functions A(z), $a_m(z)$, and $b_m(z)$ into appropriate series (e.g., Fourier series and/or power series) in the z-direction with unknown coefficients, constraining the coefficients, if necessary,to satisfy the geometric boundary conditions (eqs. (35) and (39)). The variations $\delta A(z)$, $\delta a_m(z)$, and $\delta b_m(z)$ called for in equation (65) will come from simultaneous variations in these coefficients. With the series and their variations substituted into equations (65) through (73), the requirement that δ(TPE) = 0, for any and all variations in the co-

efficients of the series, will lead to a system of algebraic equations which can be solved simultaneously for the coefficients in terms of u_o, and another equation which will then give F in terms of u_o.

If this alternate procedure is used, there is no significant advantage in neglecting the longitudinal curvature terms in the strain energy expression by setting D_z and ν' equal to zero.

NUMERICAL ANALYSIS

Numerical results for stresses and stiffness were obtained for corrugated plates with the type of end attachments illustrated in figure 2(a), namely point attachments at the ends of the trough lines only. The differential equations, simplified through the neglect of the D_z and ν' terms as noted above, were used as the basis of the numerical analysis. In this section the main steps of the numerical analysis will be described, and in the following section the computed results will be given.

System of differential equations. - A finite system of differential equations is obtained by assuming that all a_n in equation (25) are identically zero for $n>M$, and all b_n in equation (38) identically zero for $n>N$. Trial calculations with successively larger values of M and N showed that for all practical purposes convergence for the stiffness is obtained with M=4 and N=3. Convergence for the maximum stresses is not quite as good as for the stiffness; however the results based on M=4 and N=3 were considered to be sufficiently good for practical use. Further details regarding the convergence will be given in the section NUMERICAL RESULTS.

For M=4 and N=3, the two sub-systems (83a) and (83b) are

$$L_A = 0$$

$$L_{a_m} = 0 \qquad \text{for } m = 1 \text{ and } 3 \tag{84a}$$

$$L_{b_m} = 0 \qquad \text{for } m = 2$$

and

$$L_{a_m} = 0 \qquad \text{for } m = 2 \text{ and } 4$$

$$L_{b_m} = 0 \qquad \text{for } m = 1 \text{ and } 3 \tag{84b}$$

respectively.

Solution of differential equations. - The solution of the sub-systems (84a) and (84b) is facilitated by the fact that v and w must be odd in z, u must be even in z, and that only even derivatives of A and a_m, and only odd derivatives of b_m, appear in these equations. The solutions may therefore be assumed in the form

$$A = RC_o \sinh(\lambda z/R)$$

$$a_1 = C_1 \sinh(\lambda z/R) \tag{85a}$$

$$a_3 = C_3 \sinh(\lambda z/R)$$

$$b_2 = RD_2 \cosh(\lambda z/R)$$

$$a_2 = C_2 \sinh(\lambda z/R)$$

$$a_4 = C_4 \sinh(\lambda z/R) \tag{85b}$$

$$b_1 = RD_1 \cosh(\lambda z/R)$$

$$b_3 = RD_3 \cosh(\lambda z/R)$$

where C_o, C_1, C_2, C_3, C_4, D_1, D_2, D_3 and λ are dimensionless undetermined constants.

Substituting the assumed solutions (85) into the differential equations (84a) and (84b), and assuming an isotropic material, that is, one with the properties

$$\begin{aligned} \nu' &= \nu \\ E' &= E \\ G' &= G = E/[2(1+\nu)] \end{aligned} \tag{86}$$

one obtains the following two sets of relationships among the undetermined coefficients, provided that $\lambda \neq 0$:

$$\begin{bmatrix} R_1\lambda^2 & R_2\lambda^2 & R_3\lambda^2 & T_2^{(3)}\lambda \\ R_2\lambda^2 & R_4\lambda^2+R_5 & 0 & S_{12}\lambda \\ R_3\lambda^2 & 0 & R_8\lambda^2+9R_5 & S_{32}\lambda \\ T_2^{(3)}\lambda & S_{12}\lambda & S_{32}\lambda & R_c\lambda^2+4R_d \end{bmatrix} \begin{bmatrix} C_o \\ C_1 \\ C_3 \\ D_2 \end{bmatrix} = \begin{bmatrix} 0 \\ 0 \\ 0 \\ 0 \end{bmatrix} \tag{87a}$$

$$\begin{bmatrix} R_6\lambda^2+4R_5 & W_1\lambda^2 & R_a\lambda & R_7\lambda \\ W_1\lambda^2 & W_4\lambda^2+16R_5 & W_2\lambda & W_3\lambda \\ R_a\lambda & W_2\lambda & R_c\lambda^2+Rd & 0 \\ R_7\lambda & W_3\lambda & 0 & R_c\lambda^2+9R_d \end{bmatrix} \begin{bmatrix} C_2 \\ C_4 \\ D_1 \\ D_3 \end{bmatrix} = \begin{bmatrix} 0 \\ 0 \\ 0 \\ 0 \end{bmatrix} \tag{87b}$$

The constants S_{mn} and $T_2^{(3)}$ appearing in the above equations have already been defined (see eqs. (61) and (62)). With

$$k \equiv \frac{1}{12}\left(\frac{t}{R}\right)^2$$

the remaining constants in equations (87a) and (87b) can be defined as follows:

$$
\begin{aligned}
R_1 &\equiv 2S^{(2)}(1+k)\\
R_2 &\equiv T_1^{(4)} + kT_1^{(9)}\\
R_3 &\equiv T_3^{(4)} + kT_3^{(9)}\\
R_4 &\equiv 2\theta\Omega_1^2 + 2kT_1^{(10)}\\
R_5 &\equiv -\pi^2 k/[\theta(1-\nu)]\\
R_6 &\equiv \left\{4\theta[T_2^{(1)}]^2\ (1+k)\right\} + 2\theta\Omega_2^2 + 2kT_2^{(10)}\\
R_7 &\equiv S_{23} + 4T_2^{(1)}\\
R_8 &\equiv 2\theta\Omega_3^2 + 2kT_3^{(10)}\\
R_a &\equiv S_{21} - 4T_2^{(1)}\\
R_c &\equiv -4\theta/(1-\nu)\\
R_d &\equiv \pi^2/(2\theta)\\
W_1 &\equiv 4\theta T_2^{(1)}\ T_4^{(1)}(1+k)\\
W_2 &\equiv S_{41} - 4T_4^{(1)}\\
W_3 &\equiv S_{43} + 4T_4^{(1)}\\
W_4 &\equiv \left\{4\theta[T_4^{(1)}]^2\ (1+k)\right\} + 2\theta\Omega_4^2 + 2kT_4^{(10)}
\end{aligned}
\tag{88}
$$

Non-trivial solutions of equations (87a) and (87b) require that the determinants of the two systems vanish, which leads to characteristic equations of the following form for λ associated with systems (87a) and (87b), respectively:

$$\lambda^2(P_6\lambda^6 + P_4\lambda^4 + P_2\lambda^2 + P_o) = 0 \tag{89a}$$

$$Q_8\lambda^8 + Q_6\lambda^6 + Q_4\lambda^4 + Q_2\lambda^2 + Q_o = 0 \tag{89b}$$

where $P_o,\ldots, P_6$ and $Q_o,\ldots, Q_6$ are known coefficients.

The roots of equation (89a) will be denoted by ± 0, $\pm\lambda_2$, $\pm\lambda_3$, $\pm\lambda_4$. The non-zero roots λ_2, λ_3 and λ_4 lead to three independent solutions of the form (85a). In each such solution the relationship among the coefficients C_o, C_1, C_3 and D_2 can be obtained by solving the first three of equations (87a) for C_1, C_3 and D_2 in terms of C_o, with λ replaced by λ_2, λ_3 or λ_4, depending upon which of the three solutions is being sought. The zero roots of equation (89a) indicate that there is an independent solution of equations (84a) of a form other than (85a). To determine this special solution, one can return to the differential equations (84a) and by inspection note that these equations do indeed have the following solution which is not of the form (85a) but which has the same parity:

$$\begin{aligned} A &= R\, C_{01}(z/R) \\ a_1 &= 0 \\ a_3 &= 0 \\ b_2 &= R\, C_{01} E_{10} \end{aligned} \tag{90}$$

where

$$E_{10} \equiv -T_{32}/(4R_d)$$

and C_{01} is an arbitrary constant. Combining this special solution with the three which are of the form (85a), one obtains the following complete solution of equations (84a):

$$\begin{aligned} A &= R[C_{01}(z/R) + C_{02}\sinh(\lambda_2 z/R) + C_{03}\sinh(\lambda_3 z/R) + C_{04}\sinh(\lambda_4 z/R)] \\ a_1 &= E_1 C_{02}\sinh(\lambda_2 z/R) + E_4 C_{03}\sinh(\lambda_3 z/R) + E_7 C_{04}\sinh(\lambda_4 z/R) \\ a_3 &= E_2 C_{02}\sinh(\lambda_2 z/R) + E_5 C_{03}\sinh(\lambda_3 z/R) + E_8 C_{04}\sinh(\lambda_4 z/R) \\ b_2 &= R[C_{01}E_{10} + E_3 C_{02}\cosh(\lambda_2 z/R) + E_6 C_{03}\cosh(\lambda_3 z/R) + E_9 C_{04}\cosh(\lambda_4 z/R) \end{aligned} \tag{92a}$$

where C_{01}, C_{02}, C_{03}, C_{04} are arbitrary constants, and E_1 through E_9 are known quantities. They are the ratios of determinants formed from certain matrices of the elements of equations (87a) with λ replaced by λ_2, λ_3 or λ_4. They arise in solving the first three of equations (87a) for C_1, C_3 and D_2 in terms of C_o with λ equated successively to λ_2, λ_3 and λ_4.

The roots of equations (89b), all non-zero, will be denoted by $\pm\lambda_5$, $\pm\lambda_6$, $\pm\lambda_7$, and $\pm\lambda_8$. They give rise to four independent solutions of the form (85b). When these are combined, one obtains the following complete solution of equations (84b):

$$a_2 = C_{25}\sinh(\lambda_5 z/R) + C_{26}\sinh(\lambda_6 z/R) + C_{27}\sinh(\lambda_7 z/R) + C_{28}\sinh(\lambda_8 z/R)$$

$$a_4 = E_1' C_{25}\sinh(\lambda_5 z/R) + E_4' C_{26}\sin(\lambda_6 z/R) + E_7' C_{27}\sinh(\lambda_7 z/R) + E_{10}' C_{28}\sinh(\lambda_8 z/R)$$

$$b_1 = R[E_2' C_{25}\cosh(\lambda_5 z/R) + E_5' C_{26}\cosh(\lambda_6 z/R) + E_8' C_{27}\cosh(\lambda_7 z/R) + E_{11}' C_{28}\cosh(\lambda_8 z/R)]$$

$$b_3 = R[E_3' C_{25}\cosh(\lambda_5 z/R) + E_6' C_{26}\cosh(\lambda_6 z/R) + E_9' C_{27}\cosh(\lambda_7 z/R) + E_{12}' C_{28}\cosh(\lambda_8 z/R)] \quad (92b)$$

where C_{25}, C_{26}, C_{27} and C_{28} are arbitrary constants, and E_1' through E_{12}', like E_1 through E_9, are the ratios of certain determinants; they are obtained in the course of solving three of equations (87b) for C_4, D_1 and D_3 in terms of C_2 with λ replaced by λ_5, λ_6, λ_7 and λ_8 successively. The three equations selected for this calculation were the first, third, and fourth of (87b).

Satisfaction of boundary conditions. - Equations (92a) and (92b) constitute the general solution of the system of differential equations (84a) and (84b). The eight unknowns C_{01} through C_{04} and C_{25} through C_{28} will be determined from the boundary conditions. The boundary conditions are in two groups: the geometric boundary conditions and the natural boundary conditions.

For the case under consideration, (35a.1) is the only geometric boundary condition. Taking into account the fact that all a_n with n>4 are being con-

sidered to be zero, and that we have already imposed antisymmetry on $A(z)$ and $a_n(z)$, it becomes

$$-A(b) + R[-\Omega_1 a_1(b) + 2\Omega_2 a_2(b) - \Omega_3 a_3(b)] = 0 \tag{93}$$

The natural boundary conditions for the case under consideration are equations (82). Considering the definitions in equations (70) through (73), and the fact that D_z and ν' are being taken as zero (in order to neglect the longitudinal curvature terms in the strain energy expression), the first two of equations (82) are identically satisfied. Considering in addition the truncation being employed in the series (25) and (38) for $f(s,z)$ and $u(s,z)$, the rest of equations (82) become

$$b_1'(b) = 0 \quad , \quad b_2'(b) = 0 \quad , \quad b_3'(b) = 0 \tag{94}$$

$$(B_{a_1} - \Omega_1 B_A)_{z=b} = 0 \quad , \quad (B_{a_3} - \Omega_3 B_A)_{z=b} = 0 \tag{95}$$

$$(B_{a_2} + 2\Omega_2 B_A)_{z=b} = 0 \quad , \quad (B_{a_4})_{z=b} = 0 \tag{96}$$

where, in view of equations (57) and (86),

$$B_A = GtR^2[S^{(1)} \frac{u_o}{R} + 2S^{(2)}A' + (T_1^{(4)}a_1' + T_3^{(4)}a_3')R + T_2^{(3)} \frac{b_2}{R}]$$
$$+ D_{sz}[(T_1^{(9)}a_1' + T_3^{(9)}a_3')R + 2S^{(2)}A'] \tag{97}$$

$$B_{a_1} = GtR^2(T_1^{(2)} \frac{u_o}{R} + T_1^{(4)}A' + 2\theta\Omega_1^2 a_1'R + S_{12} \frac{b_2}{R})$$
$$+ D_{sz}(T_1^{(9)}A' + 2T_1^{(10)}a_1'R) \tag{98}$$

$$B_{a_2} = GtR^2[4\theta\, T_2^{(1)}(T_2^{(1)}a_2' + T_4^{(1)}a_4')R + 2\theta\Omega_2^2 a_2'R$$
$$- 4T_2^{(1)}(\frac{b_1}{R} - \frac{b_3}{R}) + S_{21} \frac{b_1}{R} + S_{23} \frac{b_3}{R}]$$
$$+ D_{sz}[4\theta\, T_2^{(1)}(T_2^{(1)}a_2' + T_4^{(1)}a_4')R + 2T_2^{(10)}a_2'R] \tag{99}$$

$$B_{a_3} = GtR^2(T_3^{(2)} \frac{u_o}{R} + T_3^{(4)}A' + 2\theta\Omega_3^2 a_3'R + S_{32} \frac{b_2}{R})$$

$$+ D_{sz}(T_3^{(9)}A' + 2T_3^{(10)}a_3'R) \qquad (100)$$

$$B_{a_4} = GtR^2[4\theta T_4^{(1)}(T_2^{(1)}a_2' + T_4^{(1)}a_4')R + 2\theta\Omega_4^2 a_4'R$$

$$- 4T_4^{(1)}(\frac{b_1}{R} - \frac{b_3}{R}) + S_{41}\frac{b_1}{R} + S_{43}\frac{b_3}{R}]$$

$$+ D_{sz}[4\theta\, T_4^{(1)}(T_2^{(1)}a_2' + T_4^{(1)}a_4')R + 2T_4^{(10)}a_4'R] \qquad (101)$$

Equations (93) through (96) constitute eight equations from which the eight unknowns C_{01} through C_{04} and C_{25} through C_{28} can be determined in terms of u_o. These equations can be solved to obtain numerical values for the following eight dimensionless parameters:

$$C_{01}R/u_o \equiv K_1$$

$$(C_{02}R/u_o)\cosh(\lambda_2 b/R) \equiv K_2$$

$$(C_{03}R/u_o)\cosh(\lambda_3 b/R) \equiv K_3$$

$$(C_{04}R/u_o)\cosh(\lambda_4 b/R) \equiv K_4$$

$$(C_{25}R/u_o)\cosh(\lambda_5 b/R) = K_5 \qquad (102)$$

$$(C_{26}R/u_o)\cosh(\lambda_6 b/R) = K_6$$

$$(C_{27}R/u_o)\cosh(\lambda_7 b/R) = K_7$$

$$(C_{28}R/u_o)\cosh(\lambda_8 b/R) = K_8$$

Determination of stiffness. - Equation (80), in conjunction with (66), (92a), (92b) and (102), gives the following relationship between the shear force F and the relative shearing displacement parameter u_o:

$$\frac{F}{Gtu_o} = b/(R\theta) + S^{(1)}K_1 b/R$$
$$+ [S^{(1)} + T_1{}^{(2)}E_1 + T_3{}^{(2)}E_2]\, K_2 \tanh\,(\lambda_2 b/R)$$
$$+ [S^{(1)} + T_1{}^{(2)}E_4 + T_3{}^{(2)}E_5]\, K_3 \tanh\,(\lambda_3 b/R)$$
$$+ [S^{(1)} + T_1{}^{(2)}E_7 + T_3{}^{(2)}E_8]\, K_4 \tanh\,(\lambda_4 b/R) \qquad (103)$$

The quantity $F/(Gtu_o)$ given by equation (103) is a dimensionless measure of the shear stiffness. From it any other dimensional or dimensionless shear stiffness measures can be determined.

Determination of strains. - It is anticipated that of the two strains ε_t and ε_ℓ, the former will be of much greater magnitude and its maximum value will occur at the extreme fibers ($\zeta=\pm t/2$) somewhere along the edges $z = \pm b$. The expression for evaluating the extreme-fiber values of ε_t along these edges can be obtained by substituting $\zeta = t/2$ and $z = b$ into the first of equations (51), after first eliminating β via equation (25). The result is

$$[\varepsilon_t(s,b)]_{\zeta=t/2} = \frac{t}{2} \sum_{n=1}^{\infty} a_n(b)\, \frac{n\pi}{2R\theta} \cdot \sin \frac{n\pi s}{2R\theta} \qquad (104)$$

or, in a form more suitable for computing and plotting, and with terms corresponding to n>4 dropped,

$$\frac{p}{u_o} \left(\frac{t}{p}\right)^{\frac{1}{2}} [\varepsilon_t(s,b)]_{\zeta=t/2} = \frac{4\pi \sin^2\theta}{\theta} \left(\frac{t}{p}\right)^{3/2} \sum_{n=1}^{4} \left[\frac{a_n(b)R}{u_o}\right] n \sin \frac{n\pi s}{2R\theta} \qquad (105)$$

The coefficients $a_n(b)R/u_o$ are to be evaluated from equations (92a) and (92b) in conjunction with (102).

There is not much point in evaluationg the shear strains γ, given by third of equations (51), inasmuch as those strains should theoretically

become infinite at the idealized attachment points employed in the analysis. As a practical matter, one would have to estimate the actual stress conditions at the attachment points by taking into account the actual nature and finite size of the attachments.

NUMERICAL RESULTS

Using equations (103) and (105), numerical results for stiffness and extreme-fiber flexural strain were obtained for a wide variety of geometries for the case of point attachments at the ends of the trough lines, assuming a Poisson's ratio of 0.3. The calculations were programmed in FORTRAN IV WATFIV and performed on the IBM 360/50 computer. The results will now be presented and discussed.

Results for shear stiffness. - The results for shear stiffness can be most efficiently presented in terms of a dimensionless shear stiffness parameter Ω. This parameter is defined as the ratio of the shear stiffness measure F/Gtu_o, as given by equation (103), to the corresponding shear stiffness measure in the case of continuous end attachments of such a nature as to produce a state of uniform shear stress throughout the corrugation . Such a state of stress would, in principle, be developed if the ends of the corrugations were continuously attached to diaphragms which were perfectly rigid with regard to deformations in their own planes, but perfectly flexible with regard to deformations normal to their planes. With such end attachments the straight-line generators of the corrugations would merely slide longitudinally with respect to each other and the shape of the cross sections would be preserved. Corresponding to a relative sliding of $2u_o$ per corrugation, the homogeneous shear strain in such a case would be simply $2u_o/p'$, where p' is the

developed width ($4R\theta$) of one corrugation. The shear force F' required on every longitudinal section in order to maintain this sliding would therefore be

$$F' = \frac{2u_o}{p'} \cdot G \cdot t \cdot 2b$$

whence

$$\frac{F'}{Gtu_o} = \frac{4b}{p'} = \frac{b}{R\theta}$$

Thus, division of equation (103) by $b/(R\theta)$ gives the dimensionless shear stiffness parameter Ω. Having a numerical value of Ω, one can recover F/Gtu_o as follows:

$$\frac{F}{Gtu_o} = \Omega \cdot \frac{b}{R\theta} = \Omega \cdot \frac{b}{p} \cdot \frac{p}{R} \cdot \frac{1}{\theta} \qquad (106)$$

Using equations (1b), one can put this result into the following alternative form:

$$\frac{F}{Gtu_o} = \Omega \cdot \frac{4(2b/p)}{[(p/h) + 4(h/p)] \tan^{-1}(2h/p)} \qquad (107)$$

Figure 8 shows a typical set of computed curves of Ω versus b/p (or L/2p). The cross section to which figure 8 applies is defined by θ=1.1612 radians = $66^{o}32'$, implying an h/p ratio of .328. (These are the proportions of some commercially available corrugated sheeting.) As is to be expected, as b/p becomes large Ω approaches unity; however, b/p must be extremely large (probably beyond the range of practicality) before unity becomes an acceptable approximation for Ω. For the larger ratios of thickness to pitch, Ω is seen to approach unity faster than for the smaller ratios, as b/p increases.

Figure 8 also shows that the curves of Ω versus b/p for different t/p values have nearly the same shape, and therefore they can be made nearly to

coincide by incorporating into the abscissa parameter some function of t/p. The appropriate modified abscissa parameter is found to be $(b/p)\ (t/p)^{3/2}$. By plotting Ω versus this parameter, the curves for all different t/p values (but fixed h/p) fall within a narrow band, as shown in figure 9.

By employing the same plotting technique as in figure 9, one can summarize the results for various h/p ratios in a single graph, figure 10. Figure 10 shows that, all other things being equal, the flatter the corrugation (i.e., the smaller the h/p) the larger will be the Ω.

It should be mentioned that h/p = 0.5 corresponds to $\theta = 90^{\circ}$, a special case to which the general analysis presented earlier does not apply. Rather than develop the special analysis and computing program for $\theta = 90^{\circ}$, it was decided to use the general analysis for $\theta = 89^{\circ}$ and 91° and average the results. The curves given in figure 10 for h/p = 0.5 were obtained in this manner.

The six bands of figure 10 are seen to have a similar shape. This suggests that a further coalescence of the results into a single band can be accomplished by incorporating h/p into the abscissa. The coalescence which results from using $(b/p)\ (t/p)^{1.5}/(h/p)^{1.6}$ as the abscissa parameter is shown in figure 11, where no attempt is made to distinguish the individual curves. If the exponent 1.6 is changed to 1.5, the somewhat simpler abscissa parameter $(b/p)\ (t/h)^{1.5}$ is obtained at the expense of a slight widening of the scatter band, as shown in figure 12.

Figure 11 or 12 is recommended as the most expeditious way of obtaining Ω, provided that one can tolerate the uncertainty represented by the vertical thickness of the scatter band. For greater accuracy one should interpolate among the curves of figure 10.

As noted earlier, the numerical analysis leading to figures 9 through 12 was based on a solution with M = 4 and N = 3; that is, all of the unknown functions were taken to be zero except A(z), $a_o(z)$ through $a_4(z)$, and $b_1(z)$ through $b_3(z)$. In order to check whether these terms were sufficient for practical convergence, conputations of Ω were also made using smaller values of M and N. The curves of Ω versus $(b/p)(t/p)^{3/2}$ for two cross sectional geometries and various sets of values of M and N are shown in figures 13(a) and (b). (The N=0 case in figure 13(a) refers to a calculation in which all the b_n of equation (38) were taken as zero.) In both figures the results for approximations 5 and 6 are indistinguishable from each other. It was therefore judged that convergence of Ω had been essentially achieved with approximation 6, i.e., M = 4, N = 3.

Results for maximum flexural strain. - The parameter appearing on the left-hand side of equation (105) is proportional to the extreme-fiber flexural strain $[\varepsilon_t(s,b)]_{\zeta=t/2}$ in the end cross section, z=b. Equation (105) was used to evaluate this parameter for a series of closely spaced values of s in order to determine its maximum absolute value. A typical variation of this parameter with respect to s is shown in figure 14. As indicated in this figure, the points of maximum flexural strain were found to be approximately at $s = \pm(25/16)R\theta$; thus each such point is in a trough and lies about midway between an attachment point and a crest-to-trough junction point.

The absolute values of the maximum extreme-fiber strain parameter for a wide range of geometries are summarized in figure 15. Because of the particular parameters employed as ordinate and abscissa, the curves for different t/p values are fairly close together, thus facilitating interpolation with respect to t/p. Since u_o, rather than F, appears in the ordinate parameter in figure 15, it is evident that these curves are best suited to the situation in which one wishes to find the maximum extreme-fiber flexural strain $\varepsilon_{t\ max}$ resulting

from a given value of the apparent overall shear strain, $2u_o/p$. Using figure 15 in conjunction with figure 9, 10 or 11, however, one can find instead the maximum flexural strain resulting from a given shear load F. It will be noted from figure 15(f) that calculations were made for h/p = .495 ($\theta = 89.5^o$) in place of h/p = .5 ($\theta = 90^o$); this was done in order to avoid the special analysis and special programming that would be required for the latter case.

The results presented in figure 15 for $\varepsilon_{t\ max}$ are based on the same approximation as those presented earlier for Ω, namely M=4, N=3. The degree of convergence achieved for $\varepsilon_{t\ max}$ with this M and N is indicated in figure 16 for a particular cross-sectional geometry. It will be noted that the convergence here is not as good as it was for Ω with the same M and N. There is an appreciable difference in figure 16 between the curve for M=4, N=3 and that for M=3, N=3. If more terms were used in the calculations, the change in the curves of $\varepsilon_{t\ max}$ versus $(b/p)(t/p)^{3/2}$ would undoubtedly be discernible. It is felt, however, that further refinement in the $\varepsilon_{t\ max}$ calculation may not be warranted in view of the fact that in practice this strain is probably affected by the finite size of the attachments, which in the present analysis were taken to be mathematical points.

It is of interest to examine the possible order of magnitude of the extreme-fiber flexural strains. From figure 15 it is seen that $(p/u_o)(t/p)^{1/2}\ \varepsilon_{t\ max}$ can be of the order of unity. Thus $\varepsilon_{t\ max}/(2u_o/p)$ can be of the order of $(p/t)^{1/2}$; that is, for some geometries the maximum extreme-fiber flexural strain $\varepsilon_{t\ max}$ can be several times as large as the apparent overall shear strain $2u_o/p$, for the type of end attachments being considered here. The use of more attachments, as in figures 2(b), (c) and (d), would tend to reduce the end-cross-sectional deformations and thereby the extreme-fiber flexural strains.

In order to convert the extreme-fiber transverse flexural strain $\varepsilon_{t\ max}$ into a corresponding extreme-fiber transverse flexural stress $\sigma_{t\ max}$, it is suggested that the following formula, based on the assumption of negligible longitudinal curvature of the generators , be used:

$$\sigma_{t\ max} = \frac{E}{1-\nu^2}\ \varepsilon_{t\ max} \tag{108}$$

COMPARISON OF PRESENT THEORY AND McKENZIE'S

K.I. McKenzie, in reference 4, presented an analysis for the shear stiffness of corrugated webs with circular-arc corrugations and two types of end attachments -- point attachments in the troughs, as in figure 2(a), and point attachments at mid-height, as in figure 2(c).

There appears to be an appreciable difference between the numerical results presented by McKenzie and those computed by the present theory, for the stiffness of a web with point attachments in the troughs, which is the only case for which a numerical comparison of the two theories has been made. The discrepancy between the two theories for this case is shown in figure 17, where the solid curves are based on the present theory, and the dashed curves are from figures 3 and 6 of reference 4.

It is believed that the difference between the present results and McKenzie's is due mainly to the assumptions on which the latter results are based. The main assumption in McKenzie's theory is that the middle surface undergoes inextensional deformation (in contrast to the assumption of merely transverse inextensibility in the present theory). As a result of this assumption the straight-line generators parallel to the corrugations are forced to remain straight and unstrained, although they may undergo rigid-body movements. The shear stiffness Γ obtained on this basis is then corrected in

an approximate way for the middle-surface shear strain in order to obtain a corrected shear stiffness Γ^1. The correction is embodied in the formula

$$\frac{1}{\Gamma^1} = \frac{1}{\Gamma_o} + \frac{1}{\Gamma} \tag{109}$$

where Γ_o is the shear stiffness assuming pure homogeneous shear strain with no cross-sectional deformation. That is, the actual flexibility, $1/\Gamma^1$, is assumed to be the sum of two other flexibilities: the flexibility $1/\Gamma_o$ due to shear deformation of the middle surface with flexural deformations suppressed, and the flexibility $1/\Gamma$ due to flexural deformations with all middle surface deformations suppressed. The present theory, on the other hand, has all flexibilities (except for transverse extension) present simultaneously.

Another possible cause of the difference between the present results and McKenzie's may be the continuity conditions employed in reference 4 at the junction between a crest and a trough and already alluded to in the footnote on p. 11. As mentioned in the discussion following equation (8) of the present paper, v and β must be continuous at the junction of a trough and crest; however, ρ is discontinuous at such a junction, changing from +R to -R, or vice versa. Consequently, equation (8) dictates that $\partial w/\partial s$ must also be discontinuous there. However, equations (11) of reference 4 violate this requirement by imposing continuity of $\partial w/\partial s$ as one of the continuity conditions at the junction. Thus, McKenzie's $-\partial w/\partial y + v/R$ is discontinuous at a junction of crest and trough, in effect permitting a kink to develop there. Consequently, his quantity $-\partial^2 w/\partial y^2 + (1/R)\,\partial v/\partial y$ is infinite at the junctions and should make an infinite contribution to the

strain energy (eq. (8) of ref. 4). McKenzie seems to have avoided this result by not integrationg the strain-energy density across the junction. By permitting kinks to develop but not integrating the strain-energy density across the kinks, it appears that McKenzie may be solving a somewhat different problem, namely the shearing of a corrugated web with crests and troughs hinged together along their junctions.

It is difficult to assess what the sense of the discrepancy should be between the present results and McKenzie's. If the surmise just above, regarding the hinges, is correct, on that score alone McKenzie's stiffnesses should be lower than the present ones. However, McKenzie's assumption of inextensional deformation would, on the other hand, lead to a raising of the stiffness, and his correction for middle-surface shear (eq. (109) of the present paper) would have an unknown effect. Thus, we cannot conclude that one theory or the other should lead to higher stiffnesses; and in fact figure 17 shows that, while the present stiffnesses are generally lower than McKenzie's, they can also be higher.

ILLUSTRATIVE APPLICATION

Shear stiffness. - Let us consider a hypothetical corrugated spar web, with the corrugations running vertically and fastened to the spar caps by means of a single small rivet at each end of a trough line, and with the following additional characteristics:

Young's modulus:	$E = 30{,}000{,}000$ psi.
Shear modulus:	$G = 12{,}000{,}000$ psi.
Poisson's ratio:	$\nu = .25$
Corrugation length:	$2b = 48$ in.
Pitch:	$p = 4$ in.
Depth:	$h = .4$ in.
Thickness:	$t = .04$ in.

In order to make a shear flow analysis of the box beam of which the web is a part, it is usually necessary to know the effective shear modulus, G_{eff}, of the web. The calculation of this quantity by means of figure 10 will now be demonstrated, assuming that the stresses are not so high as to invalidate the assumption of Hooke's law on which this figure is based, and neglecting any possible error due to the fact that it is based on a Poisson's ratio of 0.3, rather than 0.25.

From the given data

$$h/p = .4/4 = 0.1 \quad , \quad t/p = .04/4 = .01,$$

$$(b/p)(t/p)^{3/2} = (24/4)(.01)^{3/2} = .006.$$

Entering .006 as abscissa in figure 10, and reading the ordinate to the curve for $h/p = .1$ and $t/p = .01$, one obtains $\Omega = .66$.

Now entering $h/p = .1$ in figure 18, one obtains $\theta = .393$ radians and $p/R = 1.538$. Equation (106) then gives

$$\frac{F}{Gtu_o} = .66 \times \frac{24}{4} \times 1.538 \times \frac{1}{.393} = 15.5$$

The effective shear modulus, defined as the ratio of the average shear stress on vertical sections, $F/(2bt)$, to the apparent overall shear strain, $2u_o/p$, can now be computed as follows:

$$G_{eff} = \frac{F/(2bt)}{2u_o/p} = \frac{F}{Gtu_o} \cdot \frac{G}{4} \cdot \frac{p}{b}$$

$$= (15.5)(3,000,000)(4/24) = 7,750,000 \text{ psi}$$

It is of interest to see what the less accurate figures 11 and 12 would have given for Ω in this case. The abscissas required for the use of these figures are, respectively,

$$\frac{(b/p)(t/p)^{3/2}}{(h/p)^{1.6}} = \frac{.006}{(.1)^{1.6}} = .239$$

$$(b/p)(t/h)^{1.5} = (24/4)(.04/.4)^{1.5} = .190$$

Entering the first of these abscissas into figure 11, one obtains $\Omega = .67 \pm .03$, as compared with the more precise value of .66 determined from figure 10. Similarly, entering .190 as abscissa in figure 12, one obtains $\Omega = .66 \pm .04$. In this case the ordinate to the middle of the band in figure 11 or 12 is quite close to the correct value but its uncertainty would be ±5 or 6 percent. It should be noted that for small values of the abscissa in figure 11 or 12 the relative uncertainty in Ω can be much larger than 5 or 6 percent.

Flexural stress. - Suppose that we now wish to determine for the same web the maximum extreme-fiber transverse flexural stress, $\sigma_{t\ max}$, per 1000 pounds of applied vertical shear load F, again assuming that Hooke's law is valid.

Entering figure 15(b) with $(b/p)(t/p)^{3/2} = .006$ and $t/p = .01$, we find that

$$\frac{p}{u_o}\left(\frac{t}{p}\right)^{1/2} \varepsilon_{t\ max} = 1.005,$$

whence

$$\frac{\varepsilon_{t\ max}}{(2u_o/p)} = .502\left(\frac{p}{t}\right)^{1/2} = .502(100)^{1/2} = 5.02$$

That is, the maximum extreme-fiber flexural strain is in this case 5.02 times the apparent shear strain. Making use of the value of G_{eff} computed earlier, we have

$$\frac{2u_o}{p} = \frac{F/(2bt)}{G_{eff}} = \frac{1000/(48\times.04)}{7{,}750{,}000} = .671 \times 10^{-4}$$

Thus,

$$\varepsilon_{t\ max} = (5.02)(.671 \times 10^{-4}) = 3.37 \times 10^{-4}$$

The corresponding stress, according to equation (108), is

$$\sigma_{t\ max} = \frac{30\times10^6}{1-(1/16)} \times 3.37 \times 10^{-4} = 10{,}780 \text{ psi}$$

In contrast, the average shear stress on vertical sections, per 1000 pounds of applied shear load, is only

$$\frac{F}{2bt} = \frac{1000}{(48)(.04)} = 521 \text{ psi}$$

CONCLUDING REMARKS

A theoretical elastic analysis has been presented of a curvilinearly corrugated shear web with various arrangements of point attachments at the ends of the corrugations, the purpose of the analysis being to obtain information about the overall shear stiffness of such a web and the flexural strains that develop in it as a result of its cross-sectional deformations.

On the basis of this analysis, numerical results for stiffness and maximum flexural strain were computed and presented for a wide range of geometries and one kind of end attachment, namely point attachments at the ends of the trough lines. The numerical results for stiffness show that the discretely attached web can have a markedly lower stiffness than the continuously attached web, even for large values of the length-to-pitch ratio of the corrugations. The stiffness results differ appreciably from those obtained by McKenzie for the same problem. The numerical results for the maximum extreme-fiber flexural strains at the ends of the corrugations show that these strains can be considerably larger than the apparent overall shear strain of the web, and the corresponding flexural stress can be much larger than the average middle-surface shear stress.

In the analysis the crests and troughs were assumed to be identical circular arcs for simplicity. In order to apply the results to a corrugation which has identical but not-quite-circular crests and troughs, it is suggested that a circular-arc corrugation with the same pitch and depth be taken as approximately equivalent to the non-circular one. However, the error involved in such a substitution cannot at present be estimated.

The present analysis and numerical results may be of use in some instances in the design of the internal spars of aerospace vehicles if corrugated shear webs are used in these spars as a means of avoiding high thermal stresses. The present work may also be of use in the civil engineering applications of corrugated sheet, namely as roofing and siding, provided that identical fastening is used in every corrugation. At present a rather sparse fastening at the corrugation ends is often employed in the civil engineering applications; in such cases the present analysis would not apply.

It should be emphasized that the data presented in this report are theoretical and based on an analysis which idealizes the attachments as mathematical points and neglects the (nonlinear) effect of any possible interference between the deformations of the end cross sections and the flanges to which they are attached. Experiments of two kinds would be desirable: First, experiments in which one tries to simulate as closely as possible the idealizations employed in the analysis, in order to confirm the basic soundness of the latter. Secondly, experiments in which one simulates practical attachment conditions, in order to see what effect such things as finite attachment size and interference have on the stiffness and stresses. Pending such experimental investigations, the quantitative results of the present analysis should be used with some discretion.

REFERENCES

1. Lin, Chuan-jui; and Libove, Charles: Theoretical Study of Corrugated Plates: Shearing of a Trapezoidally Corrugated Plate with Trough Lines Held Straight. NASA CR-1749, Aug. 1971. (Supersedes Syracuse University Research Institute Report MAE 1833-T1, May 1970.)

2. Lin, Chuan-jui; and Libove, Charles: Theoretical Study of Corrugated Plates: Shearing of a Trapezoidally Corrugated Plate with Trough Lines Permitted to Curve. NASA CR-1750, Dec. 1971. (Supersedes Syracuse University Research Report MAE 1833-T2, June 1970.)

3. Hsiao, Chen-liau; and Libove, Charles: Theoretical Study of Corrugated Plates: Shear Stiffness of a Trapezoidally Corrugated Plate with Discrete Attachments to a Rigid Flange at the Ends of the Corrugations. Syracuse University, Department of Mechanical and Aerospace Engineering, Report No. MAE 1833-T3 July 1971. (NASA CR-1966)

4. McKenzie, K.I.: The Shear Stiffness of a Corrugated Web. R.& M. No. 3342, British A.R.C., 1963.

5. Bryan, E.R.; and Jackson, P.: The Shear Behaviour of Corrugated Steel Sheeting. In "Thin Walled Steel Structures: their design and use in buildings," K. C. Rockey and H. V. Hill, eds., Crosby Lockwood (London), Gordon and Breach (N.Y.), 1969. (Proceedings of a symposium held in Sept. 1967.)

6. Rothwell, A.: The Shear Stiffness of Flat-sided Corrugated Webs. The Aeronautical Quarterly. August 1968, pp. 224-234.

7. Kraus, H.: Thin Elastic Shells. John Wiley & Sons, Inc. 1967.

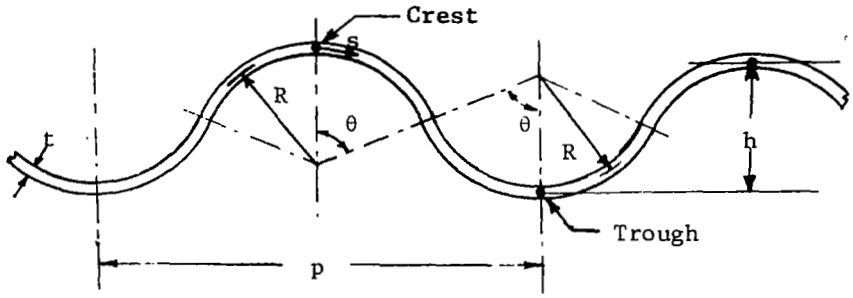

(a) Cross section

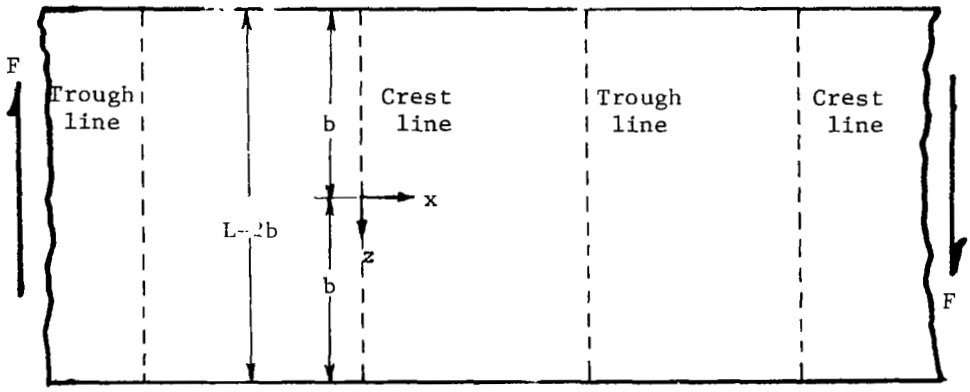

(b) Plan view

Figure 1. - Configuration and notation for curvilinearly corrugated plate in shear.

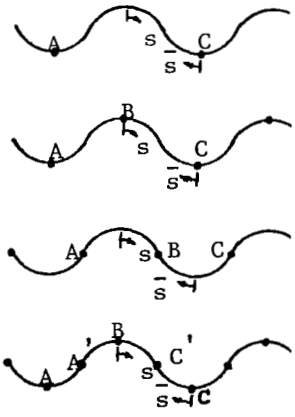

(a) Point attachments at troughs

(b) Point attachments at troughs and crests

(c) Point attachments at mid-height

(d) Point attachments at troughs, crests and mid-height

Figure 2. - Types of discrete attachment considered at ends of corrugations ($z = \pm b$).

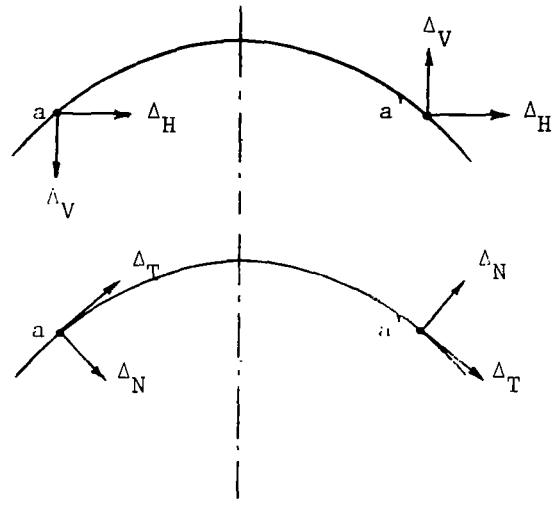

Figure 3. - Symmetry and antisymmetry of displacement components in the plane of the cross section for points symmetrically located with respect to a vertical plane of symmetry.

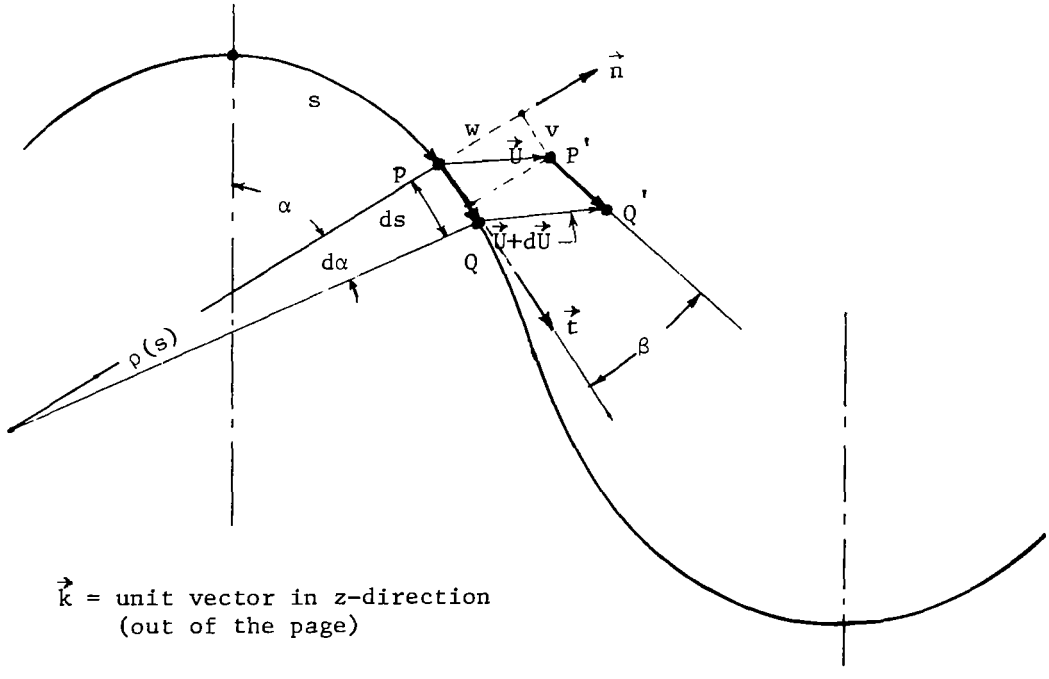

Figure 4. - Displacements, in the plane of the cross section, of middle-surface points.

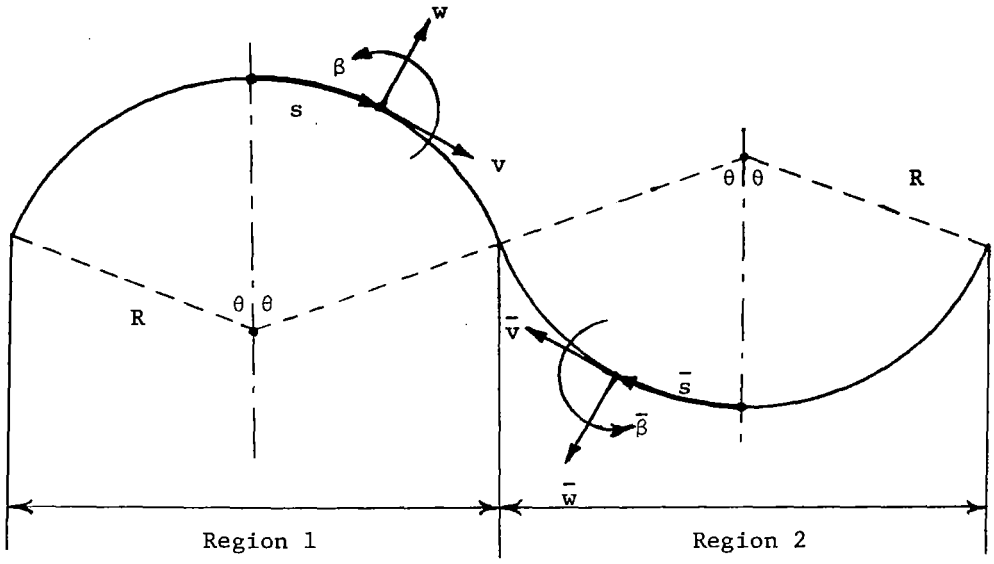

Figure 5. - Typical repeating unit of the circular-arc corrugation.

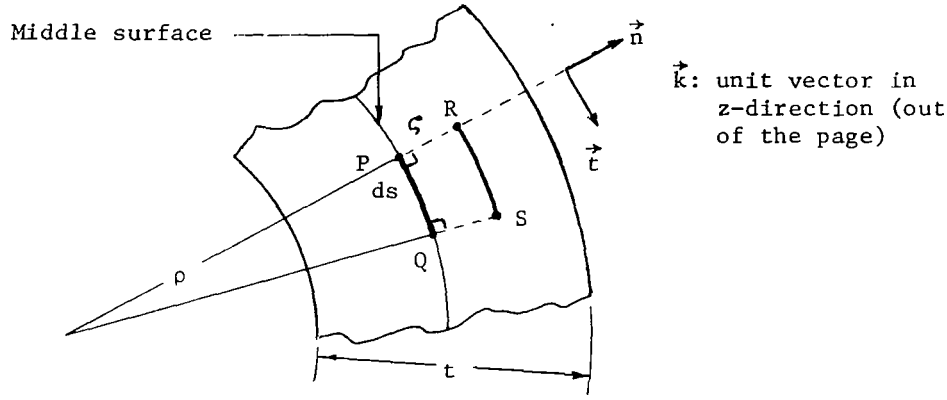

Figure 6. - Line elements PQ and RS in the cross section of the undeformed corrugation.

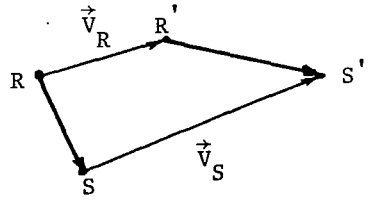

Figure 7. - Vector polygon formed by points R, S, R' and S'.

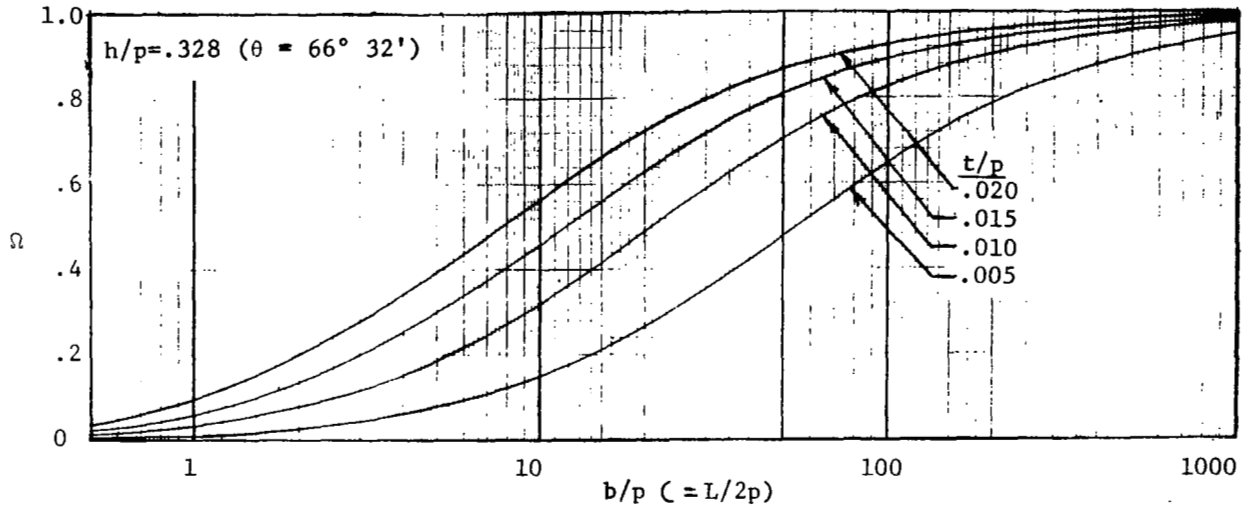

Figure 8. - Typical variation of Ω with respect to b/p.

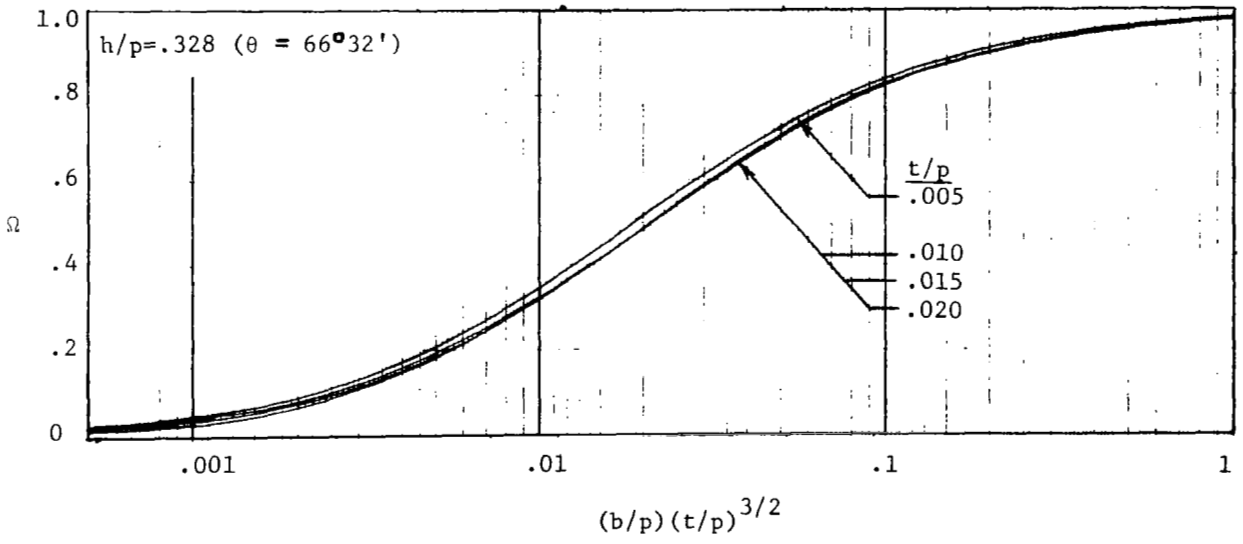

Figure 9. - Curves of Figure 8 replotted, using $(b/p)(t/p)^{3/2}$ as abscissa.

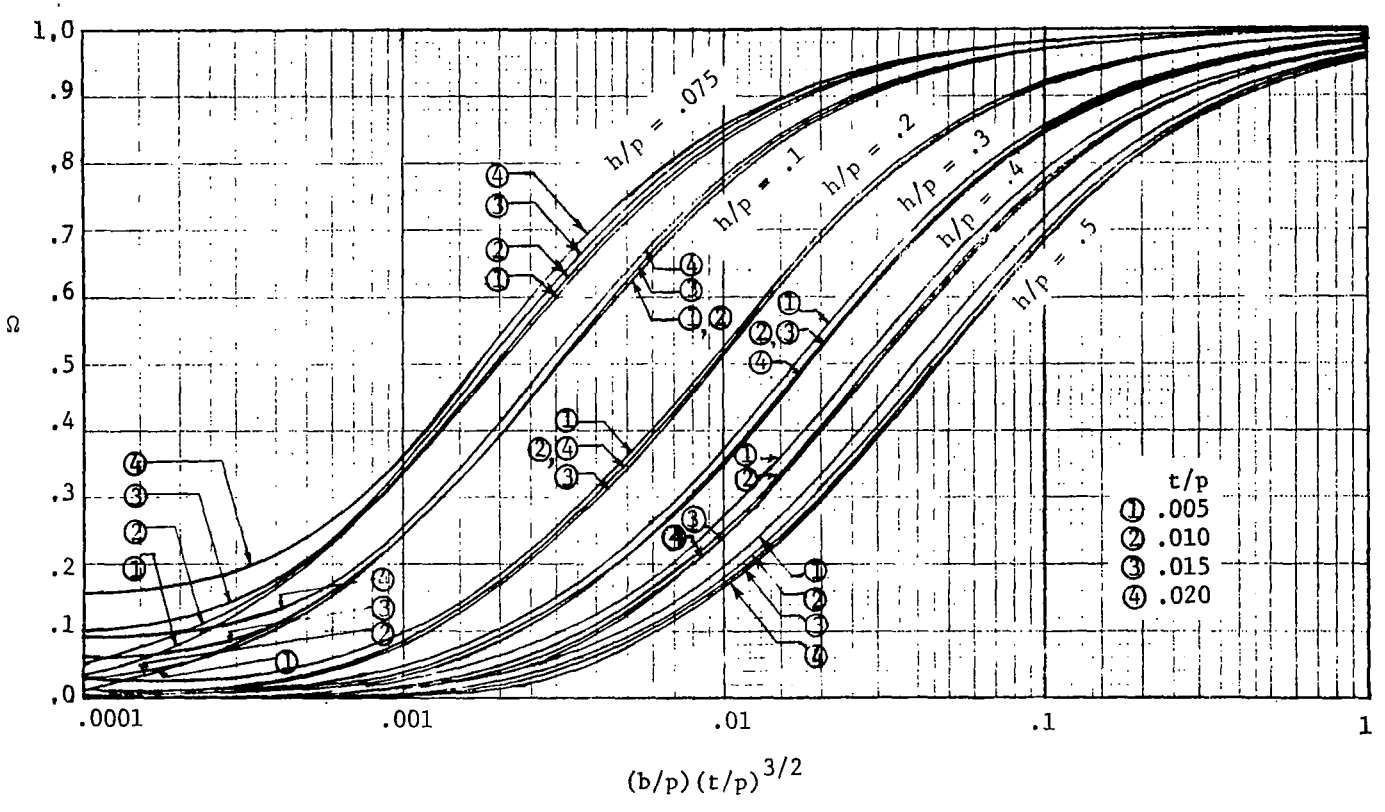

Figure 10. - Variation of Ω with respect to $(b/p)(t/p)^{3/2}$ for a series of values of h/p.

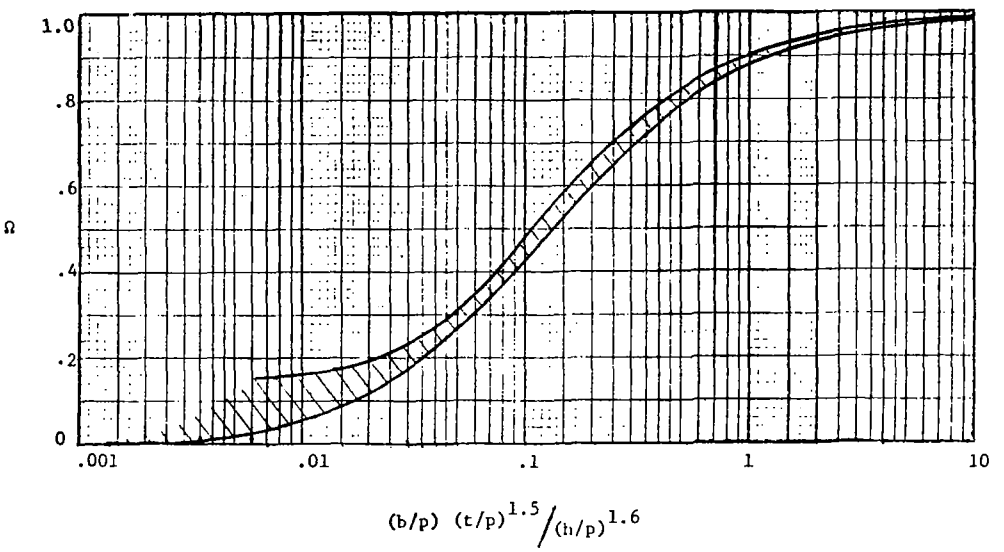

Figure 11. - Curves of figure 10 replotted with a modified abscissa parameter.

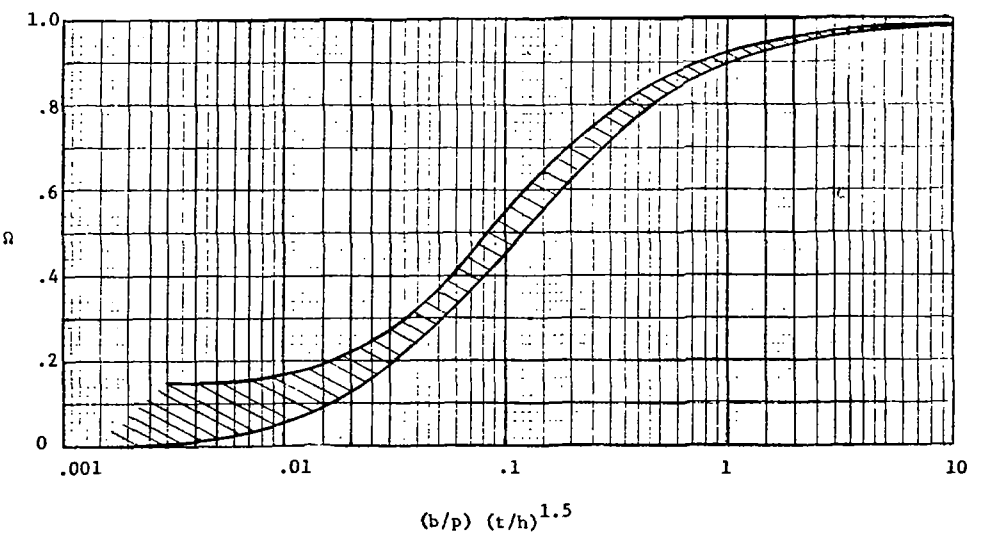

Figure 12. - Curves of figure 10 replotted with an alternate modified abscissa parameter.

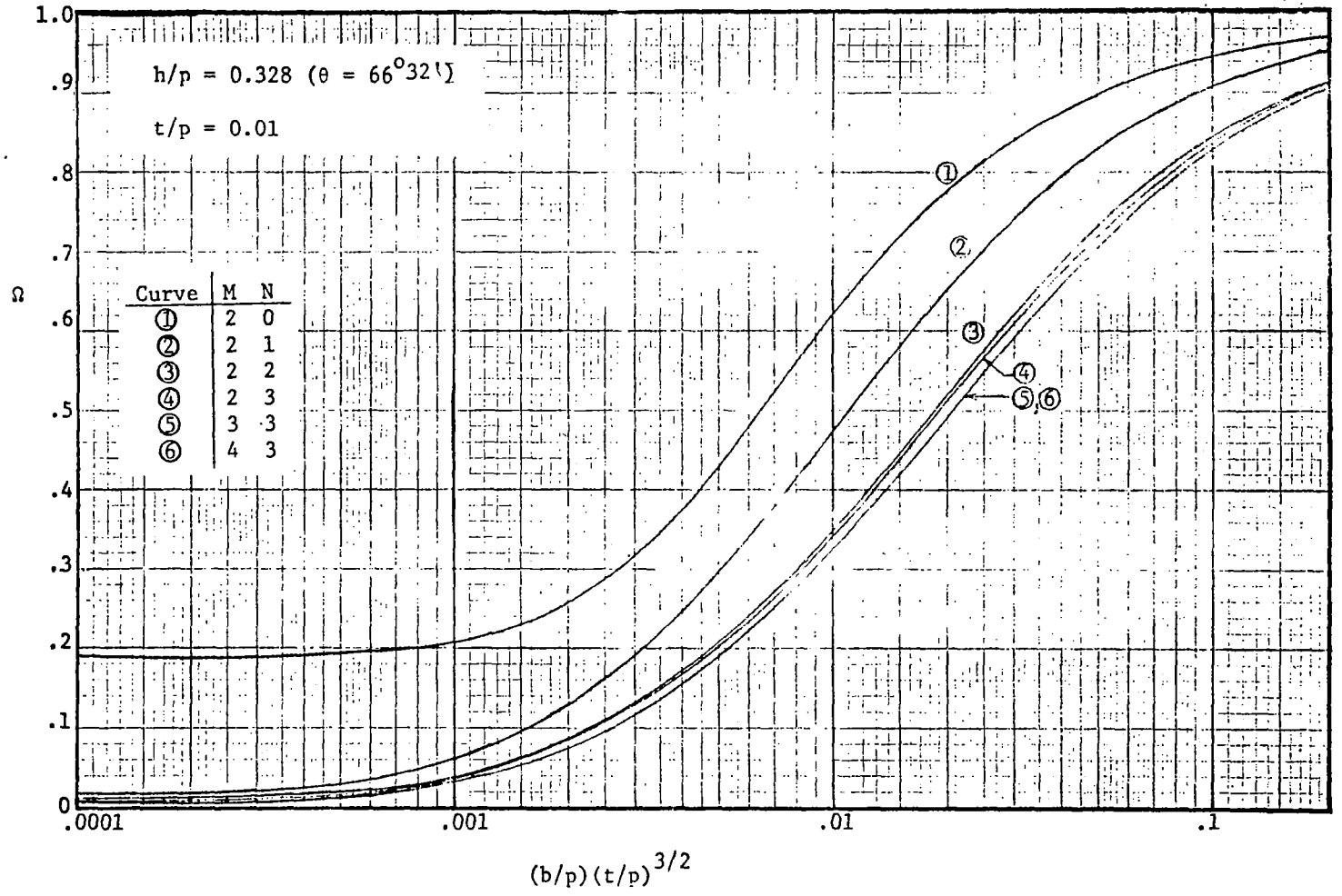

(a) h/p = 0.328 ; t/p = 0.01

Figure 13. - Study of convergence of shear-stiffness parameter Ω.

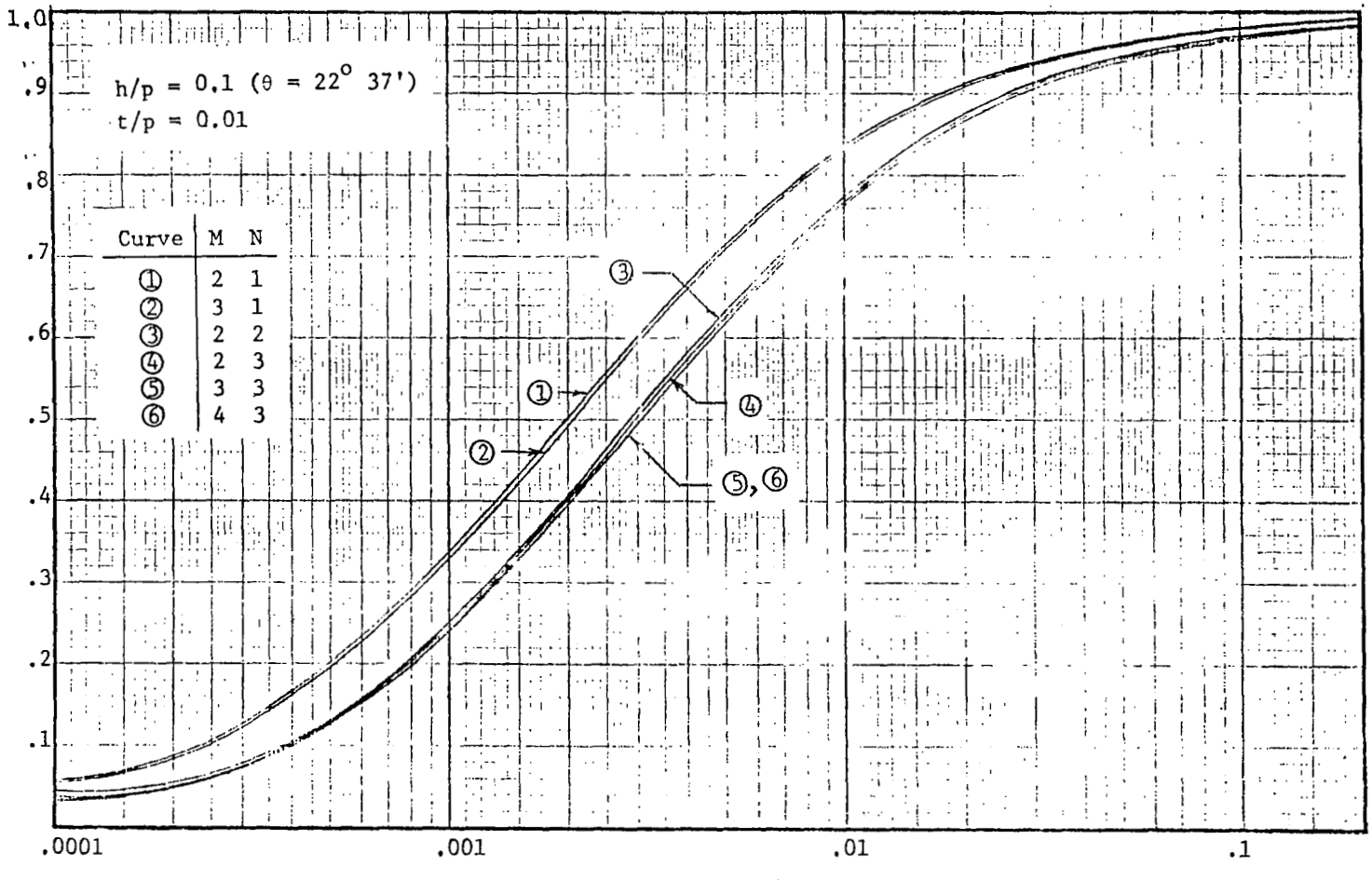

(b) h/p = 0.1 ; t/p = 0.01

Figure 13. - Concluded.

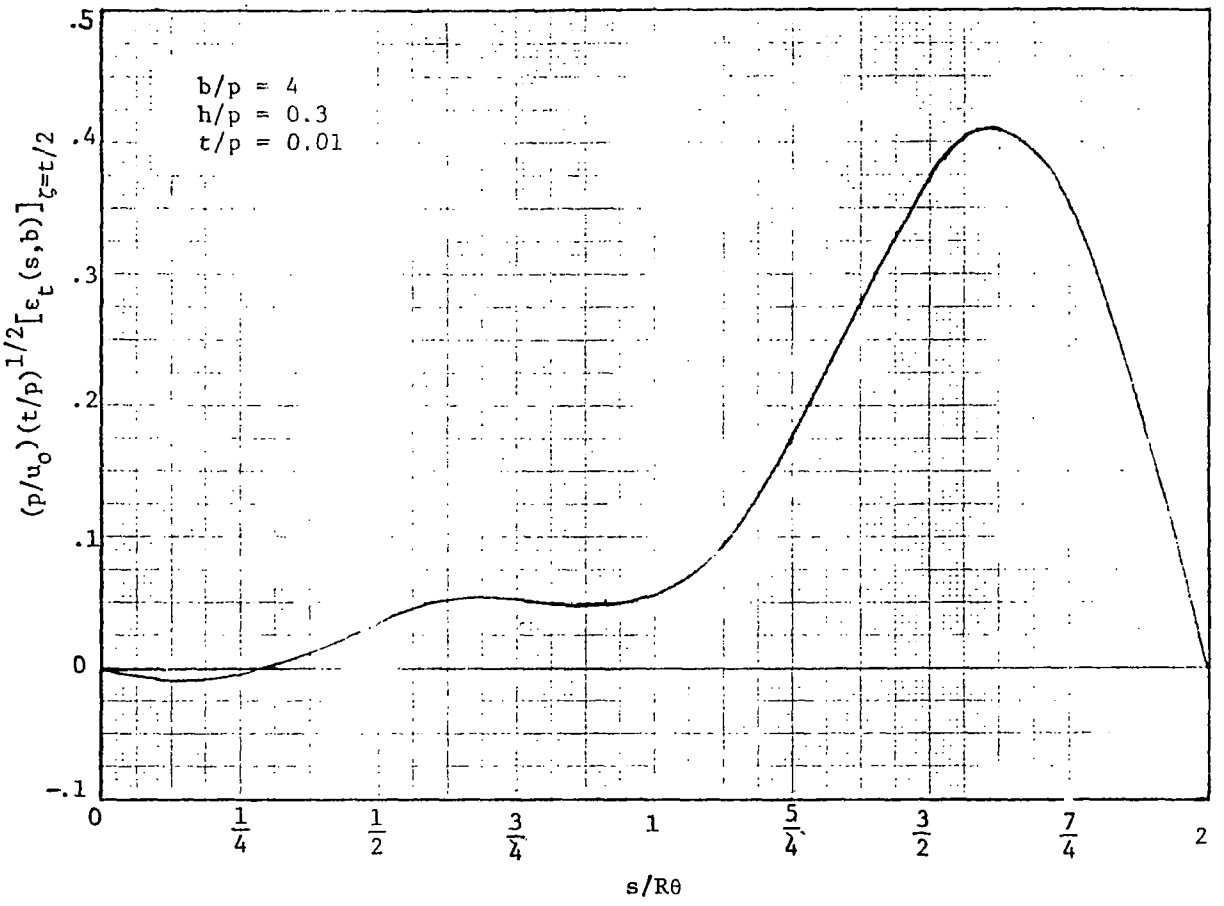

Figure 14. - Typical variation of extreme-fiber flexural strain parameter along the end cross section.

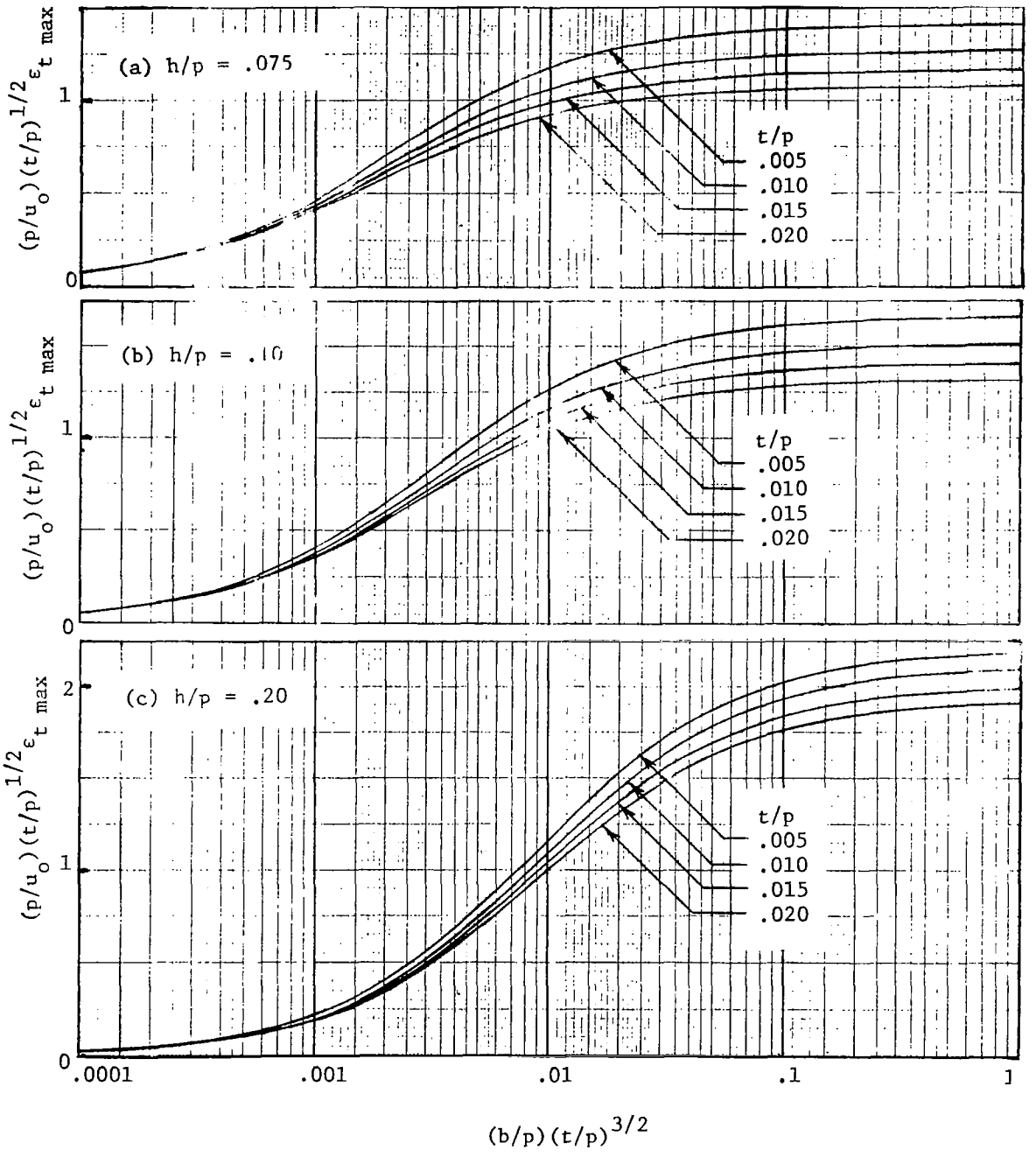

Figure 15. - Summary of computed data on maximum extreme-fiber flexural strain $\varepsilon_{t\ max}$ due to deformation of the end cross section.

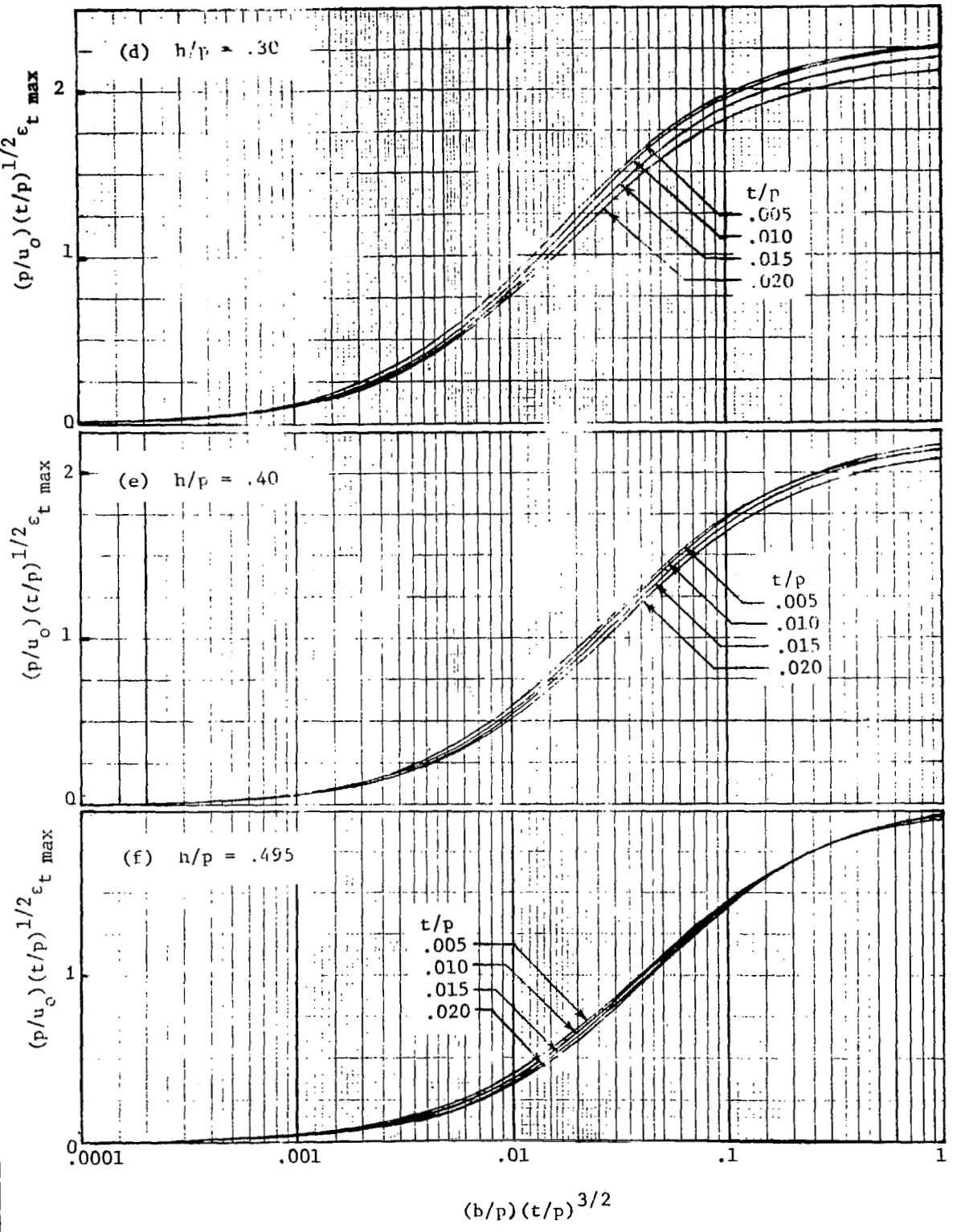

Figure 15. - Concluded.

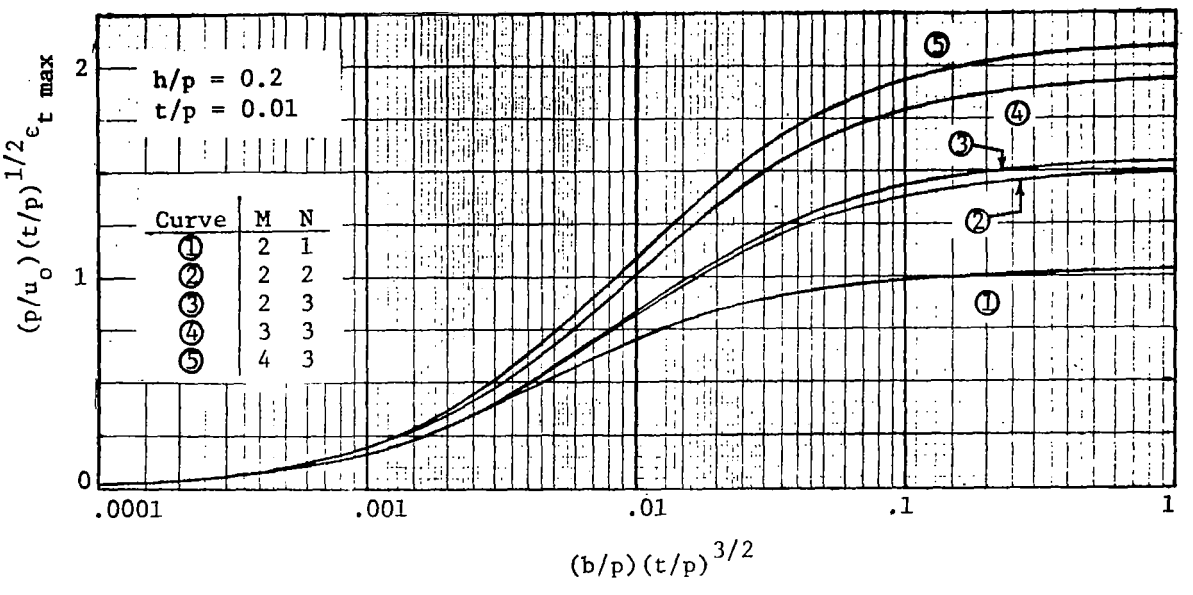

Figure 16. - Study of convergence of $\epsilon_{t\ max}$.

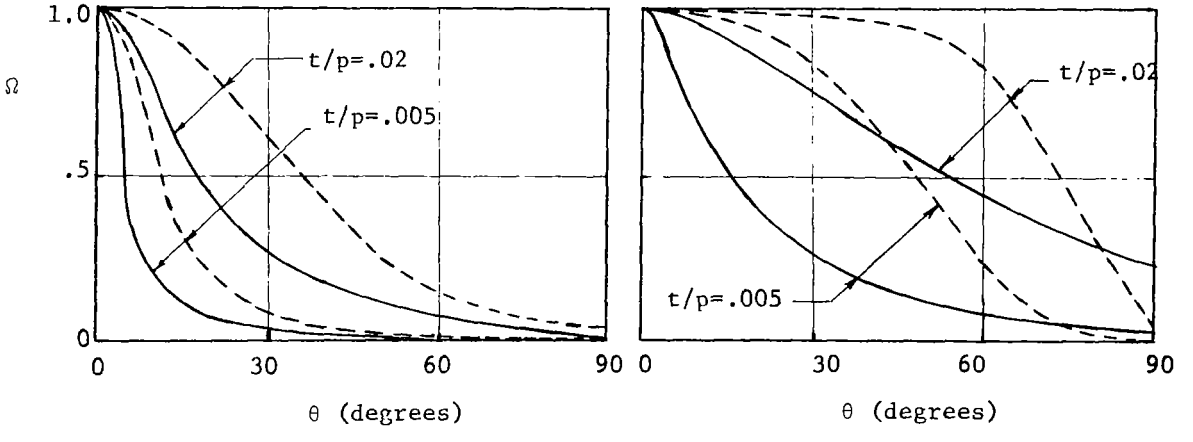

(a) b/p = .625

(b) b/p = 5

Figure 17. - Comparison of present results (solid curves) with those of reference 4 (dashed curves).

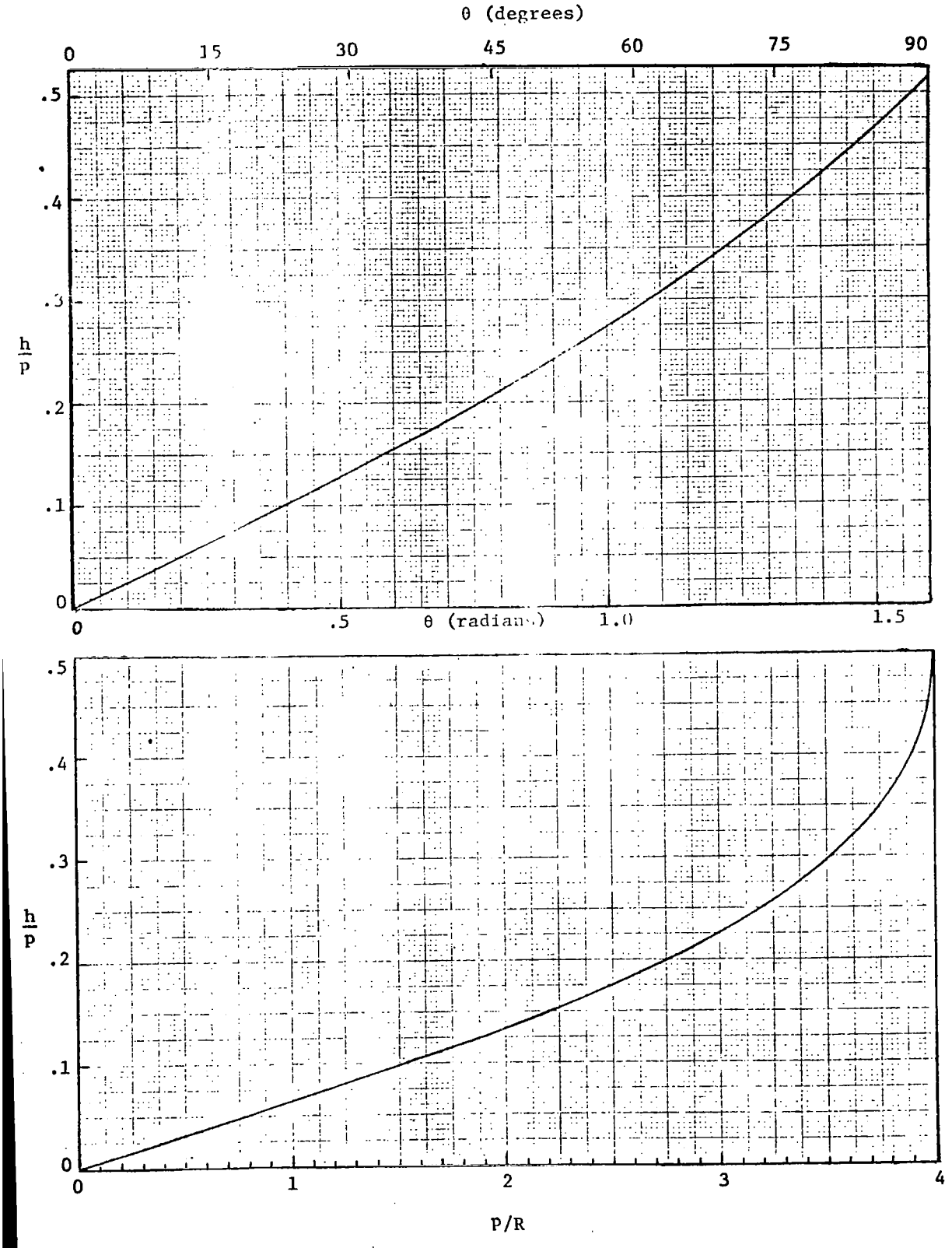

Figure 18. - Graphs of equations 1(b).